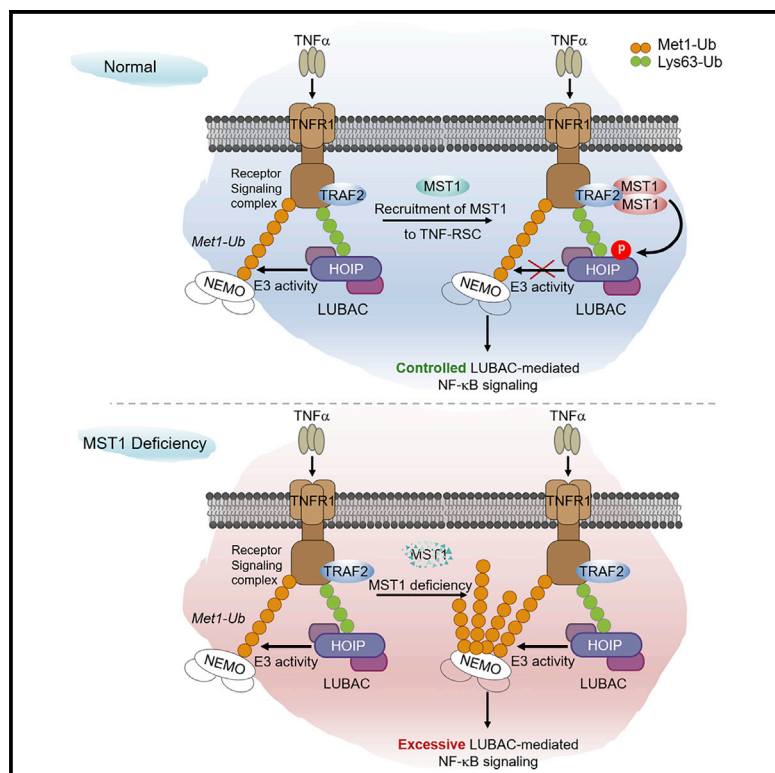


# MST1 Negatively Regulates TNF $\alpha$ -Induced NF- $\kappa$ B Signaling through Modulating LUBAC Activity

## Graphical Abstract



## Authors

In Young Lee, Jane Melissa Lim, Hyunchu Cho, ..., Je-Hyun Yoon, Hyun Kyu Song, Eui-Ju Choi

## Correspondence

ejchoi@korea.ac.kr

## In Brief

Lee et al. identify MST1 as a component of TNF-RSC that phosphorylates HOIP at serine 1,066 and thereby inhibits the linear ubiquitin chain-forming activity of LUBAC in a TRAF2-dependent manner. MST1, by inhibiting an E3 ligase activity of HOIP, negatively regulates the NF- $\kappa$ B-dependent inflammatory gene expression induced by TNF $\alpha$ .

## Highlights

- TNF $\alpha$  induces the recruitment of MST1 to the TNFR1 signaling complex (TNF-RSC)
- TRAF2 is required for the TNF $\alpha$ -induced activation of MST1 within the TNF-RSC
- MST1 phosphorylates HOIP in TNF-RSC, thereby inhibiting an E3 ligase activity of LUBAC
- MST1 attenuates the LUBAC-mediated activation of the NF- $\kappa$ B pathway

# MST1 Negatively Regulates TNF $\alpha$ -Induced NF- $\kappa$ B Signaling through Modulating LUBAC Activity

In Young Lee,<sup>1</sup> Jane Melissa Lim,<sup>1</sup> Hyuncho Cho,<sup>1</sup> Eunju Kim,<sup>1</sup> Yeonsil Kim,<sup>1</sup> Hye-Kyung Oh,<sup>1</sup> Woo Seok Yang,<sup>1</sup> Kyung-Hye Roh,<sup>1</sup> Hyun Woo Park,<sup>2</sup> Jung-Soon Mo,<sup>3</sup> Je-Hyun Yoon,<sup>4</sup> Hyun Kyu Song,<sup>1</sup> and Eui-Ju Choi<sup>1,5,\*</sup>

<sup>1</sup>Department of Life Sciences, Korea University, Seoul 02841, South Korea

<sup>2</sup>Department of Biochemistry, College of Life Science and Biotechnology, Yonsei University, Seoul 03722, South Korea

<sup>3</sup>Genomic Instability Research Center (GIRC), Ajou University School of Medicine, Suwon 16499, South Korea

<sup>4</sup>Department of Biochemistry and Molecular Biology, Medical University of South Carolina, Charleston, SC 29425, USA

<sup>5</sup>Lead Contact

\*Correspondence: [ejchoi@korea.ac.kr](mailto:ejchoi@korea.ac.kr)

<https://doi.org/10.1016/j.molcel.2019.01.022>

## SUMMARY

The nuclear factor (NF)- $\kappa$ B pathway plays a central role in inflammatory and immune responses, with aberrant activation of NF- $\kappa$ B signaling being implicated in various human disorders. Here, we show that mammalian ste20-like kinase 1 (MST1) is a previously unrecognized component of the tumor necrosis factor  $\alpha$  (TNF $\alpha$ ) receptor 1 signaling complex (TNF-RSC) and attenuates TNF $\alpha$ -induced NF- $\kappa$ B signaling. Genetic ablation of MST1 in mouse embryonic fibroblasts and bone marrow-derived macrophages potentiated the TNF $\alpha$ -induced increase in I $\kappa$ B kinase (IKK) activity, as well as the expression of NF- $\kappa$ B target genes. TNF $\alpha$  induced the recruitment of MST1 to TNF-RSC and its interaction with HOIP, the catalytic component of the E3 ligase linear ubiquitin assembly complex (LUBAC). Furthermore, MST1 activated in response to TNF $\alpha$  stimulation mediates the phosphorylation of HOIP and thereby inhibited LUBAC-dependent linear ubiquitination of NEMO/IKK $\gamma$ . Together, our findings suggest that MST1 negatively regulates TNF $\alpha$ -induced NF- $\kappa$ B signaling by targeting LUBAC.

## INTRODUCTION

The nuclear factor (NF)- $\kappa$ B signaling pathway plays a key role in the regulation of inflammatory and immune responses. In the canonical NF- $\kappa$ B pathway, proinflammatory cytokines, such as tumor necrosis factor  $\alpha$  (TNF $\alpha$ ) and interleukin (IL)-1 $\beta$ , induce activation of the canonical I $\kappa$ B kinase (IKK) complex, which is composed of the kinase subunits IKK $\alpha$  (IKK1) and IKK $\beta$  (IKK2), as well as the regulatory subunit NEMO (IKK $\gamma$ ). The activated IKK complex phosphorylates the NF- $\kappa$ B inhibitor I $\kappa$ B $\alpha$  and thereby promotes its ubiquitination and proteasomal degradation. Given that NF- $\kappa$ B is present in the cytosol of resting cells as an inactive complex with I $\kappa$ B, the degradation of the latter protein results in the release of NF- $\kappa$ B and its translocation to the nu-

cleus, where it activates transcription of various target genes (Vallabhapurapu and Karin, 2009). The NF- $\kappa$ B signaling pathway is regulated by various types of post-translational modification, including ubiquitination (Chen, 2012).

Protein ubiquitination is mediated by three enzymes: a ubiquitin (Ub)-activating enzyme (E1), a Ub-conjugating enzyme (E2), and a Ub ligase (E3) (Pickart, 2001). Ub contains seven internal lysine residues (K6, K11, K27, K29, K33, K48, and K63), each of which as well as the NH<sub>2</sub>-terminal methionine residue (M1) can serve as a link in the formation of polyubiquitin chains. Protein ubiquitination regulates many biological processes in a manner dependent on the type of Ub linkage. In the case of Ub lysine linkages, an isopeptide bond is formed between the COOH-terminal carboxyl group of the activated Ub molecule and the  $\epsilon$ -amino group of a lysine residue in the Ub moiety attached to the substrate (Pickart, 2001). In the case of linear Ub linkage, the COOH-terminal carboxyl group of Ub molecule is attached to the  $\alpha$ -amino group of M1 of the target Ub (Tokunaga and Iwai, 2012).

The linear ubiquitin assembly complex (LUBAC) is a linear ubiquitination-specific E3 ligase composed of the catalytic component HOIP and the regulatory components Sharpin and HOIL-1L (Gerlach et al., 2011; Ikeda et al., 2011; Kirisako et al., 2006; Tokunaga et al., 2011). LUBAC contributes to the regulation of both innate immunity (Damgaard et al., 2012; Ikeda et al., 2011; Inn et al., 2011; Zak et al., 2011; Zhang et al., 2008) and adaptive immunity (Gerlach et al., 2011; Hostager et al., 2010, 2011; Ikeda et al., 2011; Tokunaga et al., 2009, 2011). At the molecular level, LUBAC was initially shown to regulate TNF $\alpha$  receptor 1 (TNFR1) signaling (Haas et al., 2009; Rahighi et al., 2009; Tokunaga et al., 2009). TNF $\alpha$  triggers the recruitment of TNFR-associated factor 2 (TRAF2) and cellular inhibitor of apoptosis protein (c-IAP) to the cytosolic region of TNFR1, which is associated with TNFR-associated death-domain protein (TRADD) and receptor-interacting protein 1 (RIP1) to form the TNFR1 signaling complex (TNF-RSC) (also known as complex I) (Bertrand et al., 2008; Ea et al., 2006; Micheau and Tschopp, 2003). The K-63 ubiquitination of RIP1 promotes the recruitment of LUBAC to TNF-RSC (Haas et al., 2009; Varfolomeev et al., 2012). The recruited LUBAC mediates linear ubiquitination of NEMO and RIP1 and thereby increases the stability of TNF-RSC, as well as IKK activity, leading to the activation

of NF- $\kappa$ B (Tokunaga et al., 2009). The loss of LUBAC renders TNF-RSC unstable and induces the assembly of complex II, which triggers cell death by apoptosis or necroptosis (Berger et al., 2014; Gerlach et al., 2011; Peltzer et al., 2014; Rickard et al., 2014). Genetic ablation of *HOIP* in mice causes embryonic death at embryonic day 11 to 12 as a result of abnormal TNFR1-mediated endothelial cell death (Peltzer et al., 2014).

Mammalian Ste20-like kinase 1 (MST1) [also known as serine/threonine kinase 4 (STK4)] is a serine-threonine kinase that belongs to the family of class II germinal center kinases (Creasy et al., 1996; Creasy and Chernoff, 1995). MST1 contains a catalytic domain in its NH<sub>2</sub>-terminal region, an autoinhibitory domain in its central region, and a SARAH (Salvador/RASSF1/Hippo) coiled-coil motif in its COOH-terminal region (Creasy et al., 1996; Scheel and Hofmann, 2003). It functions in the regulation of various cellular events, including cell growth, apoptosis, and stress response (Radu and Chernoff, 2009). In particular, MST1 serves as a key mediator of intracellular signaling induced by various extracellular stimuli including TNF $\alpha$  (Chae et al., 2012; Ohtsubo et al., 2008; Park et al., 2010; Rawat and Chernoff, 2015).

To better understand the relation between MST1 and TNF $\alpha$  signaling, we have now investigated the possible regulatory role of MST1 in TNF $\alpha$ -induced NF- $\kappa$ B inflammatory signaling pathway. Here, we show that TNF $\alpha$  induces the recruitment of MST1 to TNF-RSC and the consequent activation of MST1 in a TRAF2-dependent manner. Furthermore, activated MST1 mediates the phosphorylation of HOIP and thereby inhibits its linear ubiquitination activity. Thus, MST1 attenuates the LUBAC-dependent activation of the NF- $\kappa$ B signaling pathway. Our results reveal that MST1 functions as a negative regulator of TNF $\alpha$ -induced NF- $\kappa$ B signaling in the inflammatory response.

## RESULTS

### MST1 Is a Negative Regulator of TNF $\alpha$ -Induced NF- $\kappa$ B Signaling

To investigate the possible role of MST1 in regulation of the NF- $\kappa$ B signaling pathway, we examined TNF $\alpha$ -induced NF- $\kappa$ B signaling activity in wild-type (WT) and *MST1*<sup>-/-</sup> mouse embryonic fibroblasts (MEFs). The TNF $\alpha$ -induced increase in DNA-binding activity of the NF- $\kappa$ B(p65) was markedly greater in *MST1*<sup>-/-</sup> MEFs than in WT cells (Figure 1A). Furthermore, reverse transcription (RT) and real-time polymerase chain reaction (PCR) analysis revealed that deletion of the *MST1* gene in the cells enhanced the TNF $\alpha$ -induced increases in the amounts of mRNAs for NF- $\kappa$ B target genes including those for *I $\kappa$ B $\alpha$* , *IL-6*, and inducible nitric oxide synthase (*iNOS*) (Figure 1B). The TNF $\alpha$ -induced production of IL-6 and nitric oxide (NO) was also markedly enhanced in *MST1*<sup>-/-</sup> MEFs, compared with WT cells (Figure 1C). Moreover, ablation of *MST1* increased the TNF $\alpha$ -induced phosphorylation (activation) of IKK $\alpha$ / $\beta$  activity (Figure 1D). Immunoblot analysis showed that the TNF $\alpha$ -induced degradation of I $\kappa$ B $\alpha$  was more rapid (Figure 1E), and that the TNF $\alpha$ -induced phosphorylation (activation) of NF- $\kappa$ B p65 was more pronounced (Figure 1F), in *MST1*<sup>-/-</sup> cells than in WT cells. Together, these results suggested that *MST1* negatively regulates TNF $\alpha$ -induced activation of the NF- $\kappa$ B signaling pathway. In comparison, siRNA-induced

depletion of *MST2* in *Mst1*<sup>-/-</sup> MEFs did not affect TNF $\alpha$ -induced NF- $\kappa$ B signaling events such as phosphorylation and degradation of I $\kappa$ B $\alpha$  (Figure S1A), phosphorylation of NF- $\kappa$ B p65 (Figure S1B), and *IL-6* mRNA expression (Figure S1C). To further compare the actions of *MST1* and *MST2* on TNF $\alpha$ -induced NF- $\kappa$ B pathway, we transfected Flag-tagged *MST1* or *MST2* cDNAs into *MST1/2* double-knockout (dKO) HEK293A cells (Meng et al., 2015). Deficiency of both *MST1* and *MST2* enhanced the effect of TNF $\alpha$  on the phosphorylation and degradation of I $\kappa$ B $\alpha$  in *MST1/2*-dKO cells, compared with WT HEK293A cells (Figure S1D). Compared with *MST1/2*-dKO cells, TNF $\alpha$ -induced I $\kappa$ B $\alpha$  phosphorylation was reduced, and TNF $\alpha$ -induced I $\kappa$ B $\alpha$  degradation was slowed down, in the *MST1/2*-dKO cells reconstituted with Flag-MST1 (Figure S1D). Reconstitution of Flag-MST2 in *MST1/2*-dKO cells, however, did not affect those events induced by TNF $\alpha$  (Figure S1E).

### MST1 Physically Associates with HOIP

To provide insight into the cellular functions of MST1, we previously searched for MST1 binding proteins with a yeast two-hybrid assay (Yun et al., 2011) and thereby identified HOIP (also known as RNF31) as a binding partner of MST1. HOIP is the catalytic component of the linear ubiquitination E3 enzyme LUBAC, which plays a pivotal role in the regulation of TNF $\alpha$ -induced NF- $\kappa$ B signaling events (Haas et al., 2009; Peltzer et al., 2014). To confirm the interaction between MST1 and HOIP, we performed a co-immunoprecipitation assay for the two endogenous proteins in MEFs. We found that TNF $\alpha$  promoted the physical association of MST1 with HOIP in these cells (Figure 2A). *In vitro* binding assay revealed that MST1 directly bound to HOIP but not to Sharpin or HOIL-1L (Figure 2B), both of which are regulatory components of LUBAC. Additionally, MST1 directly bound to a fragment of human HOIP, HOIP(633–1,072), that includes the RING-in-between-RING (RBR) domain and the linear Ub chain determining domain (LDD), whereas it did not bind to either HOIP(1–480) or HOIP(481–632) (Figure 2C). In a separate *in vitro* binding assay, MST1 bound to HOIP(633–909), while its binding to HOIP(910–1,072) was negligible (Figure 2D). In a reciprocal binding experiment, HOIP(633–909) bound to MST1 and MST1(1–326), but not to MST1(327–487) (Figure 2E). MST1(1–326) contains a kinase domain, while MST1(327–487) contains both an autoinhibitory domain and a SARAH (or dimerization) domain.

### MST1 Inhibits the E3 Ligase Activity of LUBAC

A HOIP fragment containing the RBR and LDD domains, HOIP(RBR-LDD), is essential for the E3 ligase activity of LUBAC (Smit et al., 2012). Given that we found that MST1 binds to HOIP(RBR-LDD) (Figure 2C), we investigated the possible effect of MST1 on the E3 ligase activity of LUBAC. We examined the linear Ub chain-forming activity of LUBAC in MEFs, using an M1 linkage-specific Ub binder (M1-SUB), the construction of which was based on the UBAN domain of NEMO (Keusekotten et al., 2013). TNF $\alpha$  increased the formation of linear Ub chains in WT MEFs, and this effect was more pronounced in *MST1*<sup>-/-</sup> MEFs (Figure 3A). Immunoprecipitation of NEMO followed by immunoblot analysis of linear Ub chains also revealed that genetic ablation of *MST1* enhanced the TNF $\alpha$ -induced linear

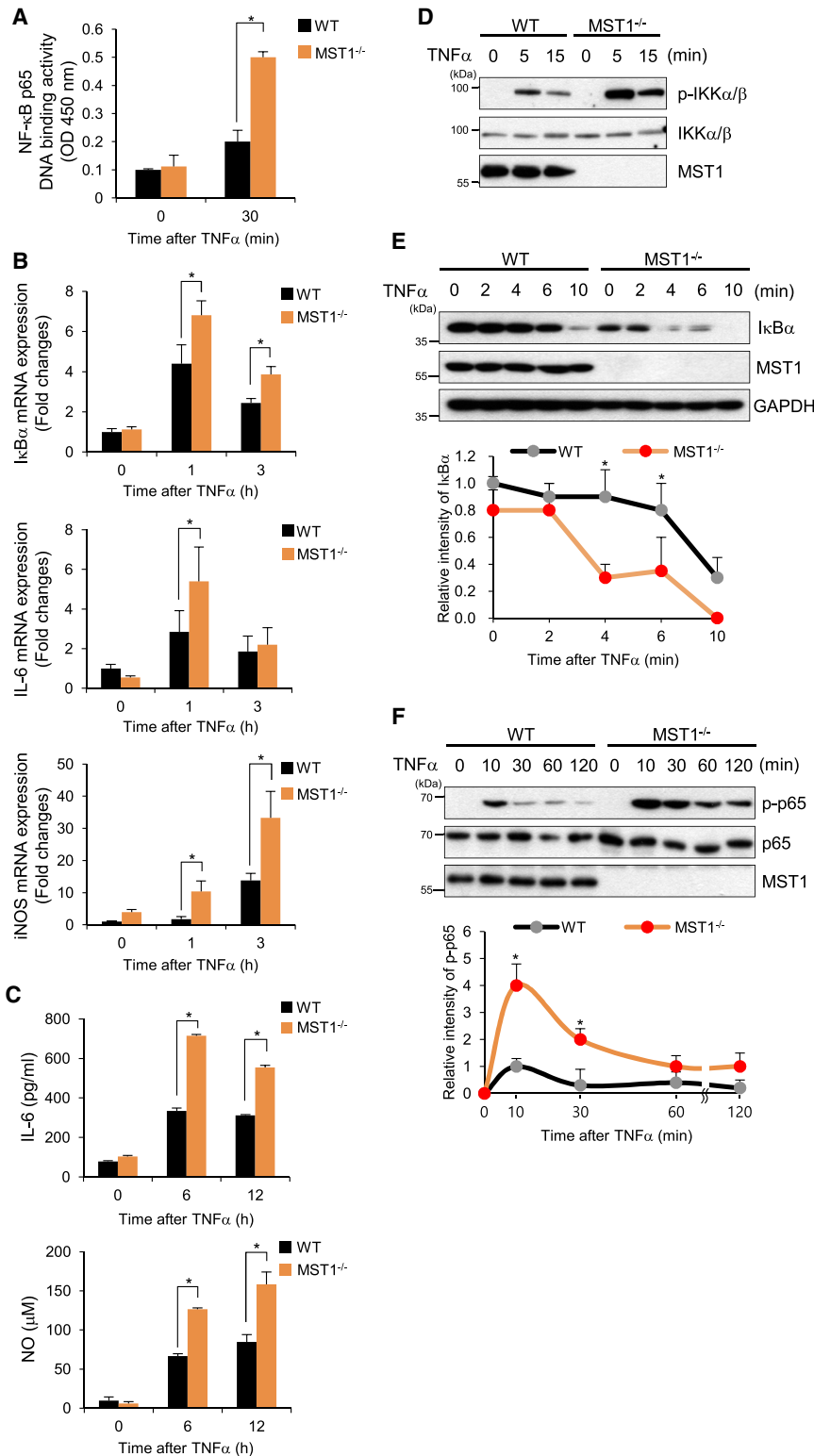


**Figure 1. Genetic Ablation of MST1 Enhances TNF $\alpha$ -Induced NF- $\kappa$ B Signaling**

(A) WT and MST1<sup>-/-</sup> MEFs were untreated or treated with 20 ng/mL TNF $\alpha$  for 30 min, after which a nuclear fraction of the lysates was assayed for the DNA-binding activity of NF- $\kappa$ B p65.

(B) qRT-PCR of *IkB $\alpha$* , *IL-6*, and *iNOS* mRNAs in WT and MST1<sup>-/-</sup> MEFs exposed to 20 ng/mL TNF $\alpha$  for 0, 1, or 3 hr.

(C) The amounts of IL-6 or NO released into culture media of WT or MST1<sup>-/-</sup> MEFs exposed to 20 ng/mL TNF $\alpha$  for 0, 6, or 12 hr were quantified with ELISA or Griess assay, respectively.

(D) WT or MST1<sup>-/-</sup> MEFs exposed to 20 ng/mL TNF $\alpha$  for the indicated times were immunoblotted with antibodies to phospho-IKK $\alpha/\beta$ , to IKK $\alpha/\beta$ , or to MST1.

(E and F) WT or MST1<sup>-/-</sup> MEFs exposed to 20 ng/mL TNF $\alpha$  were immunoblotted with indicated antibodies (upper panels). The band intensity of *IkB $\alpha$*  relative to that of GAPDH (E) or that of phospho-p65 relative to that of total NF- $\kappa$ B p65 (F) was quantified (lower panels). All quantitative data are means  $\pm$  SEM from two independent experiments. \* $p < 0.05$ . See also Figure S1.

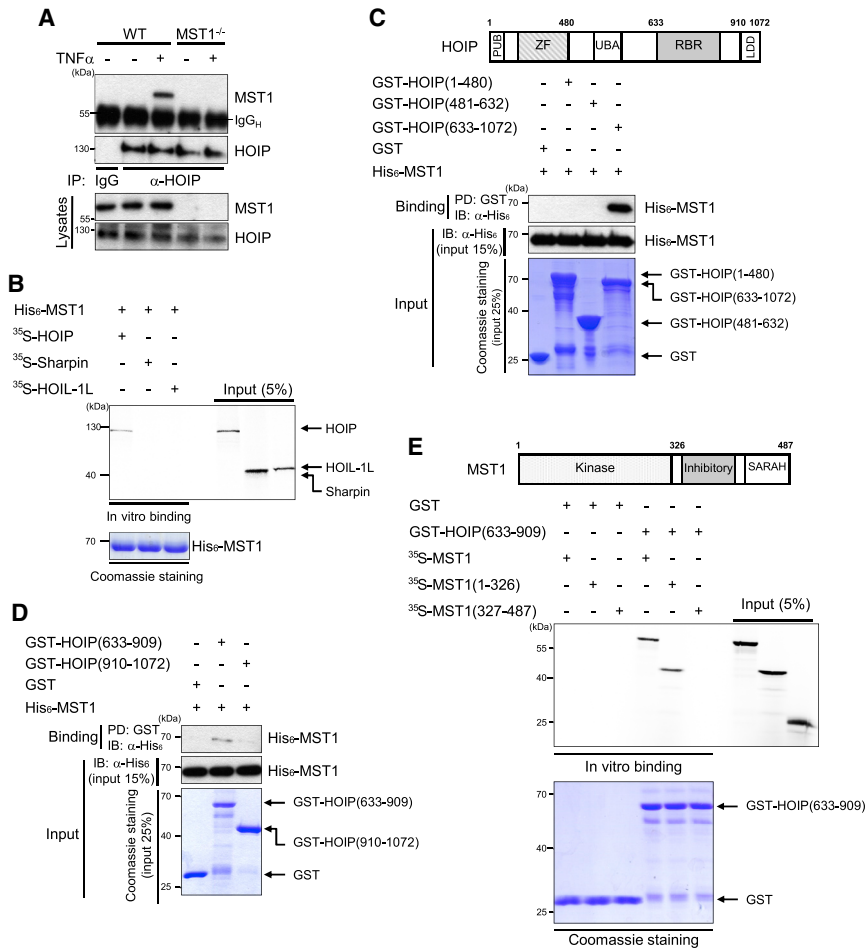


**Figure 2. Physical Interaction between MST1 and HOIP**

(A) WT and MST1<sup>-/-</sup> MEFs were untreated or treated with 20 ng/mL TNF $\alpha$  for 5 min, then immunoprecipitated with control rabbit IgG or HOIP antibody. The resulting precipitates were immunoblotted with antibodies to MST1 or to HOIP.

(B) *In vitro* assay for binding of His<sub>6</sub>-tagged MST1(K59R) to <sup>35</sup>S-labeled HOIP, Sharpin, or HOIL-1L. The reaction mixtures were pulled down with Ni-NTA beads. Bead-bound proteins were eluted and analyzed by SDS-PAGE and autoradiography. A portion (5%) of the <sup>35</sup>S-labeled protein input was also shown. The gel was also stained with Coomassie brilliant blue.

(C and D) *In vitro* assay for binding of His<sub>6</sub>-MST1(K59R) to GST-fused fragments of HOIP. The reaction mixtures were subjected to GST pull-down (PD), and bead-bound proteins were eluted and immunoblotted with anti-His<sub>6</sub> antibody. A portion (15%) of the His<sub>6</sub>-MST1(K59R) input is also shown. A portion (25%) of the GST-fused protein input was visualized with Coomassie staining.

(E) *In vitro* binding assay for GST-fused HOIP(633-909) and <sup>35</sup>S-labeled MST1 fragments. The reaction mixtures were pulled down with glutathione-agarose beads. Bead-bound proteins were eluted and analyzed by SDS-PAGE and autoradiography. A portion (5%) of the <sup>35</sup>S-labeled protein input was also shown.

ubiquitination of NEMO (Figure 3A). Together, these results suggested that MST1, by binding to HOIP, negatively regulates the TNF $\alpha$ -induced stimulation of the linear Ub chain-forming activity of LUBAC. Of note, ablation of MST1 did not affect the interaction of HOIP with Sharpin or HOIL-1L (Figure 3B).

TNF $\alpha$  induces the recruitment of LUBAC to TNF-RSC and the consequent linear ubiquitination by LUBAC of several components of TNF-RSC (Gerlach et al., 2011). Given that MST1 inhibited the TNF $\alpha$ -induced linear ubiquitination (Figure 3A), we examined whether MST1 might prevent the TNF $\alpha$ -induced linear ubiquitination within TNF-RSC. WT and MST1<sup>-/-</sup> MEFs were stimulated with a glutathione S-transferase (GST)-fused TNF $\alpha$ , and TNF-RSC was then pulled down with the use of glutathione-conjugated beads and subjected to immunoblot analysis. This analysis revealed that MST1 deficiency enhanced the TNF $\alpha$ -induced formation of linear Ub chains in TNF-RSC (Figure 3C). Immunostaining data also showed that colocalization of linear Ub chains with TNF $\alpha$  after TNF $\alpha$  stimulation was markedly increased in MST1<sup>-/-</sup> MEFs, compared with WT MEFs (Figure S2A). In comparison, the effect of MST1 deficiency on the colocalization of K63-linked Ub chains with TNF $\alpha$  was not significant (Figure S2B).

Given that MST1 negatively regulated the TNF $\alpha$ -induced formation of linear Ub chains within TNF-RSC (Figure 3C), we

examined whether MST1 might suppress the TNF $\alpha$ -induced recruitment of LUBAC components to TNF-RSC. Ablation of MST1 did not affect the TNF $\alpha$ -induced recruitment of the LUBAC components HOIP, SHARPIN, or HOIL-1L, to TNF-RSC (Figure 3D). MST1 deficiency also did not affect the TNF $\alpha$ -induced recruitment of cIAP1 or that of the deubiquitinases CYLD and A20 to TNF-RSC, whereas it increased the abundance of RIP1 within the TNF-RSC. Importantly, MST1 was also recruited to TNF-RSC in response to the stimulation of WT cells with GST-TNF $\alpha$  (Figures 3D and S2C), indicating that MST1 is a previously unrecognized component of TNF-RSC. siRNA-mediated HOIP depletion did not affect the abundance of both total and phosphorylated (activated) forms of MST1 within the TNF-RSC in MEFs, while it markedly attenuated the abundance of linear Ub chains in the TNF-RSC (Figure S2D). Furthermore, the observation that TNF $\alpha$  induces the recruitment of both MST1 and HOIP to TNF-RSC (Figure 3D) suggested that the TNF $\alpha$ -dependent interaction between MST1 and HOIP (Figure 2A) might occur within this complex. MST1 deficiency also increased the TNF $\alpha$ -induced recruitment of both total and activated forms of IKK to TNF-RSC in MEFs (Figure 3E). Unlike MST1, MST2 was not recruited to the TNF-RSC in MEFs after GST-TNF $\alpha$  treatment (Figure S2C).

Next, we examined whether MST1 directly affects the catalytic activity of HOIP. An *in vitro* ubiquitination assay revealed that the E3 ligase activity of LUBAC was markedly inhibited by MST1, but

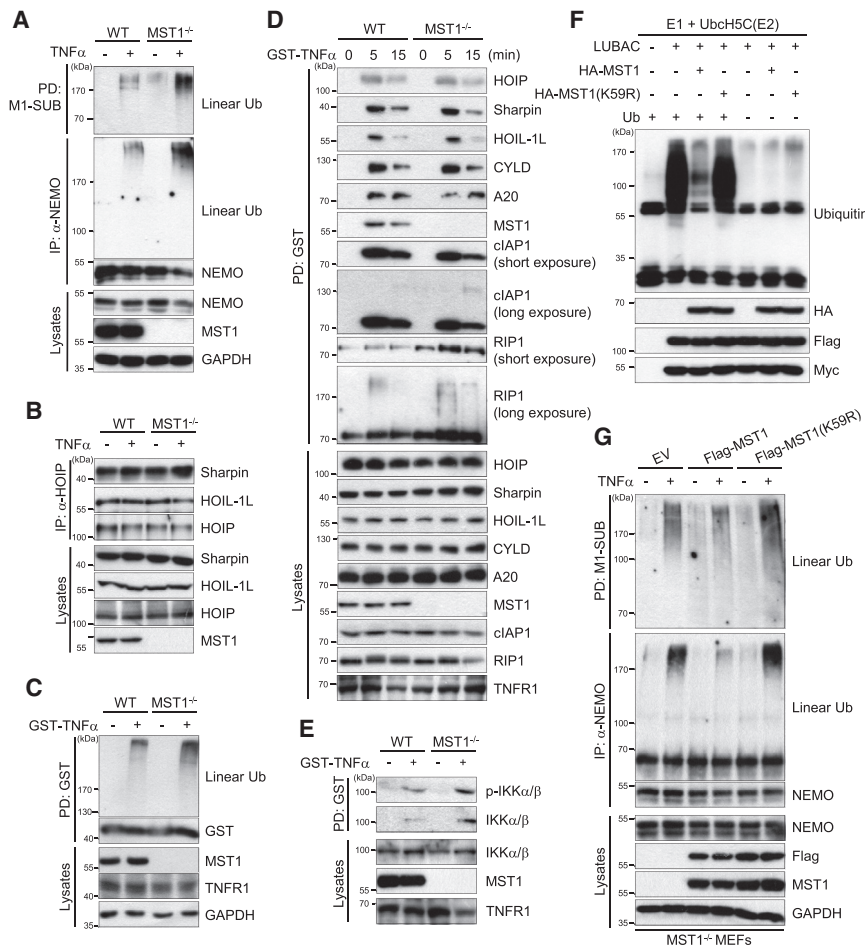


**Figure 3. MST1 Inhibits the E3 Ligase Activity of LUBAC**

(A) WT and *MST1*<sup>-/-</sup> MEFs were untreated or treated with 20 ng/mL TNF $\alpha$  for 5 min. Cell lysates were pulled down with GST-fused M1-SUB, and the resulting pellets were immunoblotted with anti-linear Ub antibody. The lysates were also immunoprecipitated with anti-NEMO antibody, followed by immunoblotting with anti-linear Ub or anti-NEMO antibody.

(B) Cell lysates prepared as in (A) were immunoprecipitated with anti-HOIP antibody, followed by immunoblotting with antibodies to Sharpin, to HOIL-1L, or to HOIP.

(C–E) WT and *MST1*<sup>-/-</sup> MEFs were untreated (C) or treated (E) with 1  $\mu$ g/mL GST-TNF $\alpha$  for 5 min or for the indicated times (D). Cell lysates were pulled down with glutathione-agarose beads, and the bead-bound proteins were immunoblotted with indicated antibodies.

(F) *In vitro* ubiquitination assay with E1, E2, LUBAC (Flag-HOIP and Myc-HOIL-1L), and Ub in the absence or presence of HA-MST1 or MST1(K59R). HA-MST1 proteins were obtained by immunoprecipitation with anti-HA antibody from corresponding transfected 293T cells.

(G) *MST1*<sup>-/-</sup> MEFs were transfected for 48 hr with a vector for Flag-MST1 or Flag-MST1(K59R) or an empty vector, then were untreated or treated with 20 ng/mL TNF $\alpha$  for 5 min. The cells were examined for linear Ub formation by a pull-down assay with GST-fused M1-SUB and for linear ubiquitination of NEMO by coimmunoprecipitation, as in (A).

See also Figure S2.

not by the K59R kinase-dead mutant of MST1 (Figure 3F). We also performed reconstitution experiments by re-expressing either wild-type MST1 or MST1(K59R) in *MST1*<sup>-/-</sup> MEFs. The effect of TNF $\alpha$  on the formation of linear Ub chains as well as on linear ubiquitination of NEMO was attenuated by expression of WT MST1, but not by that of MST1(K59R), in the *MST1*<sup>-/-</sup> cells (Figure 3G). Together, these results suggested that MST1, by binding to HOIP, inhibits the linear Ub chain-forming activity of LUBAC in a kinase activity-dependent manner.

### MST1 Phosphorylates HOIP at Ser<sup>1,066</sup> in Its LDD Region

Given our findings that MST1 binds to HOIP and inhibits the catalytic activity of HOIP, we examined whether it might mediate the phosphorylation of HOIP. pIMAGO-based analysis of protein phosphorylation revealed that TNF $\alpha$  markedly increased the phosphorylation of endogenous HOIP in WT MEFs but not in *MST1*<sup>-/-</sup> MEFs (Figure 4A). Furthermore, *in vitro* phosphorylation analysis showed that MST1 immunoprecipitates prepared from TNF $\alpha$ -treated WT MEFs were able to phosphorylate a fragment of human HOIP containing RBR and LDD (amino acids 633 to 1,072) (Figure 4B) but not HOIP(1–480) or HOIP(481–632) (Figure S3A). In comparison, MST2 did not phosphorylate HOIP(633–1,072) *in vitro* (Figure S3C).

To identify phosphorylation sites of HOIP, we analyzed the phosphorylated HOIP(633–1,072) fragment by mass spectrometry and found that Ser<sup>1,066</sup> was phosphorylated by MST1 (Figure 4C). Serine-1,066 is present in the LDD of human HOIP and is highly conserved across multiple mammalian species (Figure 4D). To confirm the phosphorylation of this site of HOIP by MST1, we prepared rabbit polyclonal antibody specific to the phosphorylated HOIP (Figure S3B). This antibody recognized HOIP phosphorylated by MST1 *in vitro*, but it did not detect a S1066A mutant form of human HOIP also subjected to the *in vitro* kinase assay (Figure S3D). Immunoblot analysis with this phospho-HOIP antibody revealed that TNF $\alpha$  treatment markedly increased the cellular abundance of phosphorylated HOIP in WT MEFs but not in *MST1*<sup>-/-</sup> cells (Figure 4E). Taken together, our results demonstrated that HOIP is a natural substrate of MST1. MST1 has been previously shown to catalyze serine phosphorylation of various proteins, including well-recognized substrates such as histone H2B (Cheung et al., 2003) and FOXO transcription factors, FOXO1 and FOXO3 (Lehtinen et al., 2006; Yuan et al., 2009).

TNF $\alpha$  stimulation promoted the phosphorylation of HOIP within TNF-RSC in WT MEFs but not in *MST1*<sup>-/-</sup> cells, while MST1 deficiency itself did not affect the TNF $\alpha$ -induced

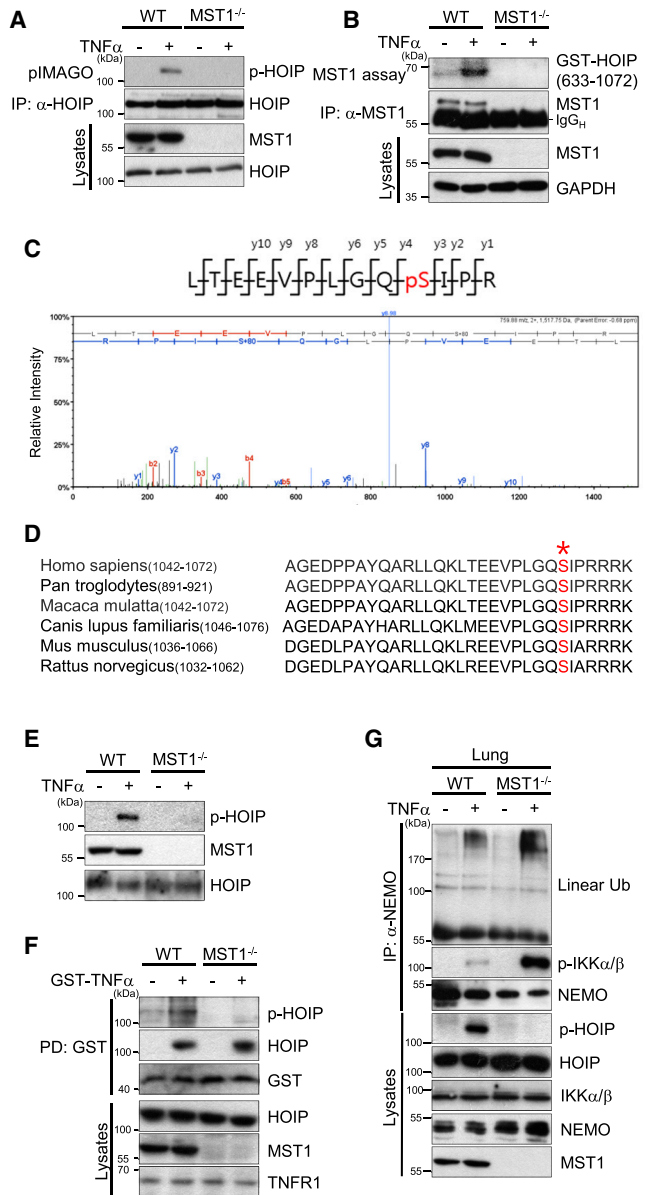


**Figure 4. MST1 Phosphorylates Human HOIP at Ser<sup>1,066</sup>**  
 (A and B) WT and *MST1*<sup>-/-</sup> MEFs were untreated or treated with 20 ng/mL TNF $\alpha$  for 10 min, and immunoprecipitated with antibodies to HOIP (A) or to MST1 (B). The HOIP precipitates were analyzed for phosphorylation with pIMAGO kit (A). The MST1 precipitates were used for an *in vitro* kinase assay with GST-HOIP(633-1072) as substrate (B).  
 (C) Identification of a phosphorylation site of HOIP by mass spectrometry.  
 (D) Sequence conservation for a phosphorylation site of human HOIP (Ser<sup>1,066</sup>, red) among various mammalian species.  
 (E) WT and *MST1*<sup>-/-</sup> MEFs were untreated or treated with 20 ng/mL TNF $\alpha$  for 10 min. Cell lysates were immunoblotted with antibodies to phospho-HOIP (Ser<sup>1,066</sup>), to HOIP, or to MST1.  
 (F) WT and *MST1*<sup>-/-</sup> MEFs were untreated or treated with 1  $\mu$ g/mL GST-TNF $\alpha$  for 10 min. The lysates were pulled down with glutathione-agarose beads, and the bead-bound proteins were immunoblotted with indicated antibodies.  
 (G) Lung extracts obtained from 8-week-old WT and *MST1*<sup>-/-</sup> mice untreated or treated with TNF $\alpha$  (125  $\mu$ g/kg) for 5 hr were immunoprecipitated with anti-NEMO antibody, followed by immunoblotting with indicated antibodies. See also Figure S3.

recruitment of HOIP to the TNF-RSC (Figure 4F). The S1066A mutation of HOIP also did not affect the recruitment of HOIP to the TNF-RSC (Figure S3E), suggesting that HOIP phosphorylation by MST1 does not modulate the recruitment of HOIP to the TNF-RSC. *In vivo* administration of TNF $\alpha$  promoted the phosphorylation of HOIP in the lung tissue from WT mice but not from *MST1*<sup>-/-</sup> mice (Figure 4G). Noticeably, the stimulating effect of TNF $\alpha$  on linear ubiquitination of NEMO as well as phosphorylation (activation) of IKK complex in the lung tissue was more pronounced in *MST1*<sup>-/-</sup> mice compared to WT mice.

### MST1-Mediated Phosphorylation of HOIP Attenuates the E3 Ligase Activity of LUBAC

We examined whether MST1-mediated phosphorylation of HOIP affects the catalytic activity of HOIP. After being phosphorylated by MST1, recombinant HOIP catalytic domain was examined for its E3 ligase activity by *in vitro* ubiquitination assay. In this assay, the MST1-mediated phosphorylation inhibited the E3 activity of the HOIP catalytic domain (Figure S4A). In additional ubiquitination assays, both WT and S1066A mutant forms of HOIP mediated the formation of linear Ub chains *in vitro* in the presence of HOIL-1L (Figure 5A). MST1 abolished the linear Ub chain formation mediated by HOIP(WT) but not that mediated by HOIP(S1066A). We next depleted MEFs of endogenous HOIP by RNA interference (RNAi) and then reconstituted the cells with ectopic human HOIP(WT) or HOIP(S1066A). TNF $\alpha$  induced the formation of linear Ub chains in the cells reconstituted with HOIP(WT) but not in non-reconstituted cells, and this effect of TNF $\alpha$  was enhanced further in the cells expressing HOIP(S1066A) (Figure 5B). Consistent with these results, the TNF $\alpha$ -induced linear ubiquitination of NEMO was more pronounced in the cells reconstituted with HOIP(S1066A) than in those reconstituted with HOIP(WT) (Figure 5C). Furthermore, TNF $\alpha$ -dependent formation of linear Ub chains as well as linear ubiquitination of NEMO was attenuated in the cells reconstituted with a phosphomimetic mutant HOIP(S1066E), compared with that of the cells reconstituted with HOIP(WT) (Figures S4B and S4C). These observations suggested that the phosphorylation of HOIP reduces the linear Ub chain-forming E3 activity of LUBAC.

The acceptor Ub interacts with the LDD of HOIP in the linear ubiquitination reaction (Smit et al., 2012). Given that Ser<sup>1,066</sup> is located in the LDD of human HOIP, we examined whether its MST1-mediated phosphorylation might affect the interaction between the LDD and linear Ub chains. An *in vitro* binding assay revealed that MBP-fused LDD of human HOIP, which contains amino acids 927-1,072 of the HOIP, interacted directly with GST-fused linear tetra-Ub chains (linear Ub<sub>4</sub>), and that this binding was abolished by prior MST1-mediated phosphorylation of MBP-HOIP(LDD) (Figure 5D). Furthermore, such prior exposure to MST1 did not affect the interaction of the S1066A mutant form of HOIP(LDD) with linear Ub<sub>4</sub> (Figure 5E). In addition, two phosphomimetic mutants, S1066D and S1066E, of HOIP(LDD) failed to interact with linear Ub<sub>4</sub> (Figure 5F). Together, these results suggested that the MST1-mediated phosphorylation of HOIP interferes with the recognition of the acceptor Ub by the LDD of HOIP.

Of note, in transfection studies using *MST1*<sup>-/-</sup> MEFs, ectopic expression of MST1 did not affect the interaction of HOIP with

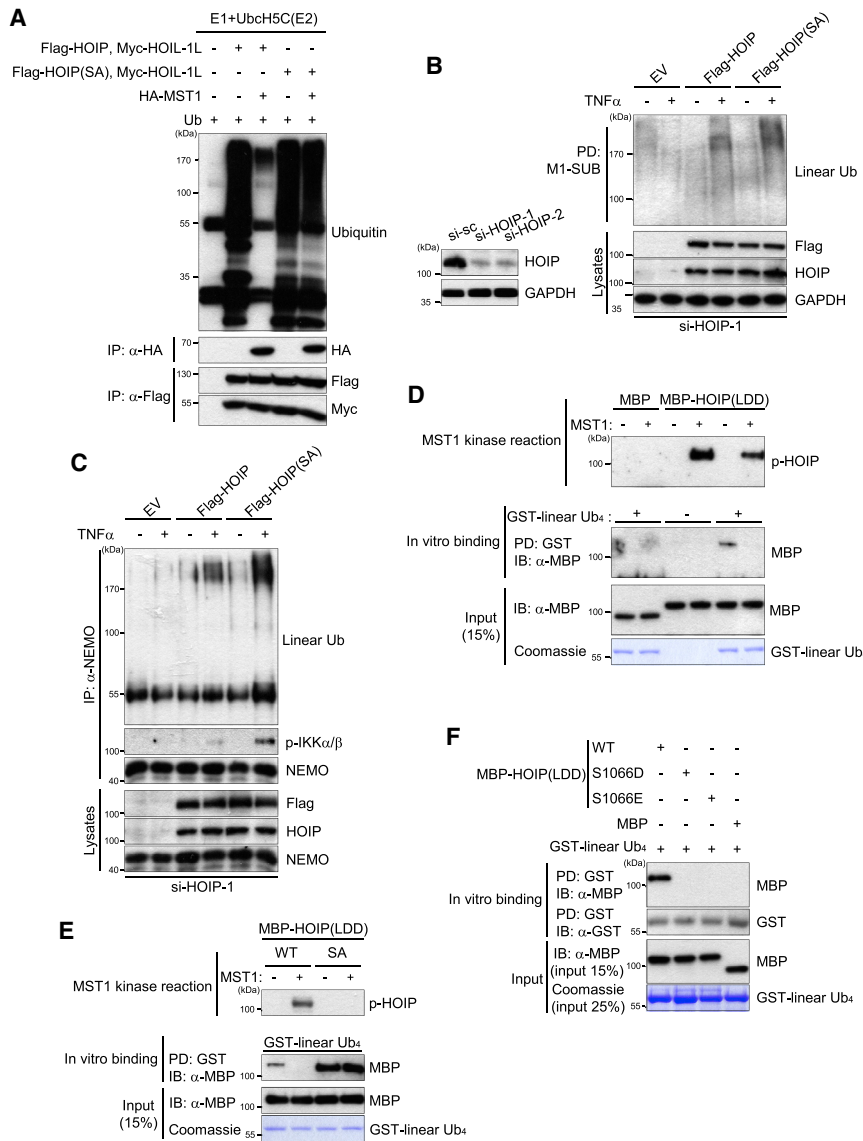


**Figure 5. Phosphorylation of HOIP by MST1 Inhibits the E3 Ligase Activity of LUBAC**

(A) *In vitro* ubiquitination assays with LUBAC [Flag-HOIP(WT or S1066A) and Myc-HOIL-1L], E1, E2, and Ub in the absence or presence of HA-MST1. HA-MST1 was obtained by immunoprecipitation with anti-HA antibody from 293T cells expressing HA-MST1.

(B and C) MEFs were transfected first for 24 hr with control (si-sc) or HOIP (si-HOIP-1 or si-HOIP-2) siRNAs and then for 24 hr with a vector for Flag-HOIP or HOIP(S1066A) or with an empty vector (EV), after which the cells were untreated or treated with 20 ng/mL TNF $\alpha$  for 5 min. Cell lysates were subjected either to pull-down with GST-fused M1-SUB followed by immunoblotting with antibody to linear Ub (B) or to immunoprecipitation with anti-NEMO antibody followed by immunoblotting with the indicated antibodies (C).

(D and E) *In vitro* phosphorylation reaction of MBP-HOIP(LDD) (D) or WT or S1066A mutant forms of MBP-HOIP(LDD) (E) was performed in the absence or presence of MST1. The phosphorylation of MBP-HOIP(LDD) was confirmed by immunoblotting with phospho-HOIP (S1066) antibody. The MBP fusion proteins were then incubated with GST-tagged linear Ub<sub>4</sub> for 1 hr at 4 $^{\circ}$ C, after which the reaction mixtures were pulled down with glutathione-agarose beads. Bead-bound proteins were immunoblotted with antibody to MBP. A portion (15%) of the GST-linear Ub<sub>4</sub> input to the binding mixtures was visualized by Coomassie staining. A portion (15%) of the MBP fusion protein input is also shown.

(F) MBP-HOIP(LDD) variants (WT, S1066D, or S1066E) or MBP alone were examined for *in vitro* binding to GST-linear Ub<sub>4</sub>, as in (E).

See also Figure S4.

OTULIN (Figure S4D) or CYLD (Figure S4E). Additionally, either expression of a constitutively active MST1 or the S1066E mutation of HOIP did not affect the binding of HOIP to OTULIN or CYLD (Figures S4F and S4G).

### TRAF2 Mediates the TNF $\alpha$ -Induced Stimulation of MST1

Next, we investigated the mechanism by which TNF $\alpha$  activates MST1. Given that TNF $\alpha$  triggers the recruitment of MST1 (Figures 3D and S2C) and TRAF2 (Hsu et al., 1996; Shu et al., 1996) to TNF-RSC and that TRAF2 was previously shown to contribute to the activation of MST1 (Roh and Choi, 2016), we examined the action of TRAF2 on TNF $\alpha$ -induced MST1 activation. Co-immunoprecipitation analysis revealed that TNF $\alpha$  induced the physical interaction of TRAF2 with MST1, but not with MST2, in MEFs (Figure 6A). Moreover, TRAF2 deficiency abolished the stimulating effect of TNF $\alpha$  on the phosphorylation (activation) (Figure 6B) as well as the kinase activity (Figure S5A)

of MST1, suggesting that TRAF2 mediates the TNF $\alpha$ -induced activation of MST1. TNF $\alpha$ -induced interaction between MST1 and HOIP was detected by co-immunoprecipitation using cell lysates containing the TNF-RSC, but not by that using cell lysates depleted of TNF-RSC (Figure S5B), implicating that the MST1-HOIP interaction induced by TNF $\alpha$  stimulation occurs mainly in the TNF-RSC. Given that TNF $\alpha$ -induced recruitment of MST1 to the TNF-RSC was abolished in TRAF2 $^{-/-}$  MEFs (Figure S5C), we next examined whether TRAF2 is required for the MST1-HOIP interaction within the TNF-RSC. TNF-RSC analysis data indicated that TRAF2 deficiency prevented the TNF $\alpha$ -induced binding between MST1 and HOIP within TNF-RSC in TRAF2 $^{-/-}$  MEFs (Figure 6C). Our results suggested that TRAF2 mediates the TNF $\alpha$ -induced recruitment of MST1 to TNF-RSC and consequent interaction between MST1 and HOIP within the TNF-RSC.

The homo-dimerization of MST1 was previously shown to contribute to its TRAF2-mediated activation (Roh and Choi,

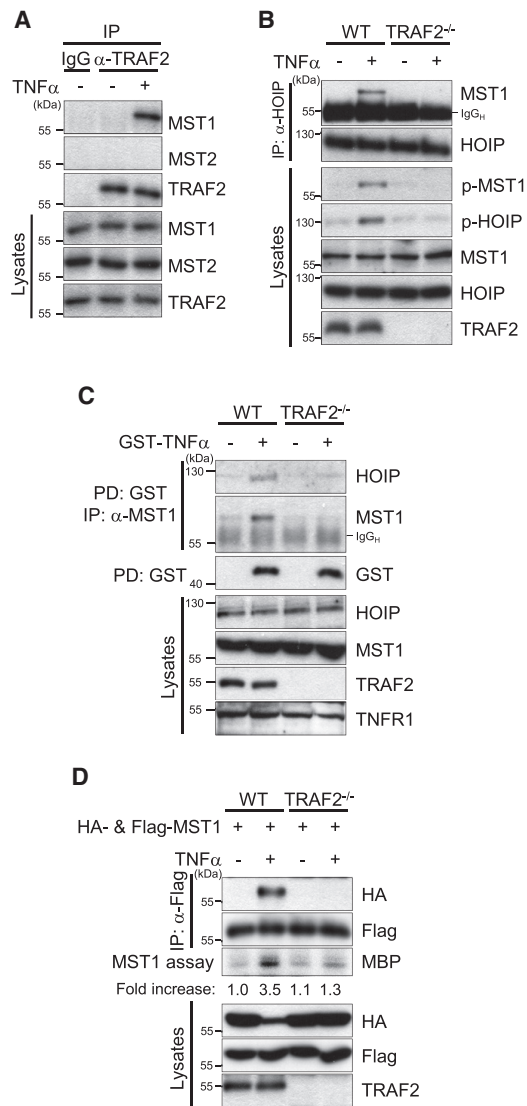


**Figure 6. TRAF2 Mediates TNF $\alpha$ -Induced MST1 Activation**

(A) MEFs untreated or treated with 20 ng/mL TNF $\alpha$  for 5 min were immunoprecipitated with TRAF2 antibody or rabbit IgG, followed by immunoblot analysis with antibodies to MST1, to MST2, or to TRAF2.

(B) WT or TRAF2<sup>-/-</sup> MEFs were untreated or treated with 20 ng/mL TNF $\alpha$  for 5 min. Cell lysates were immunoprecipitated with HOIP antibody, followed by immunoblotting with antibodies to MST1 or to HOIP. Cell lysates were also immunoblotted with antibodies to phospho-MST1, to phospho-HOIP, to MST1, to HOIP, or to TRAF2.

(C) WT or TRAF2<sup>-/-</sup> MEFs were untreated or treated with 1  $\mu$ g/mL GST-TNF $\alpha$  for 5 min, and then were subjected to TNF-RSC pull-down assay using glutathione-agarose beads. Bead-bound proteins were immunoprecipitated with anti-MST1 antibody, followed by immunoblotting with antibodies to HOIP or to MST1.

(D) WT or TRAF2<sup>-/-</sup> MEFs were transfected for 48 hr with plasmids for HA-MST1 and Flag-MST1, and then were untreated or treated with 20 ng/mL TNF $\alpha$  for 5 min. Cell lysates were immunoprecipitated with Flag antibody, followed by immunoblotting with HA or Flag antibodies. The Flag precipitates were also assayed for MST1 activity with myelin basic protein as substrate.

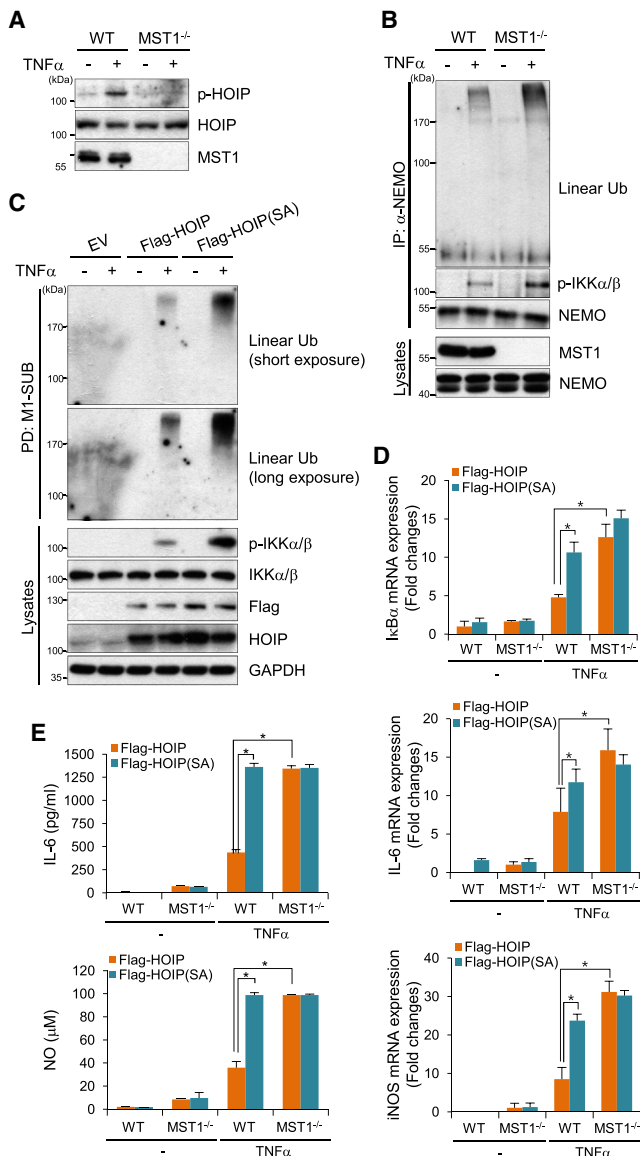
See also Figure S5.

2016). Therefore, we examined whether TNF $\alpha$  might induce the TRAF2-dependent homo-dimerization of MST1. Co-immunoprecipitation analysis of WT or TRAF2<sup>-/-</sup> MEFs transfected with vectors for Flag-MST1 and hemagglutinin epitope (HA)-tagged MST1 revealed that TNF $\alpha$  induced the homo-dimerization and activation of MST1 in the WT cells but not in the TRAF2<sup>-/-</sup> cells (Figure 6D). We also examined MST1 homo-dimerization with a proximity ligation assay (PLA) in WT or TRAF2<sup>-/-</sup> MEFs transfected with vectors encoding Flag-MST1 and Myc-MST1. TNF $\alpha$  was found again to induce MST1 homo-dimerization in WT cells but not in TRAF2<sup>-/-</sup> cells (Figure S5D), indicating that TRAF2 is required for the TNF $\alpha$ -induced homo-dimerization of MST1. In the PLA experiments, red fluorescent dots reflect the binding between Flag-MST1 and Myc-MST1. TRAF2(272–501), which is a TRAF2 mutant unable to bind to MST1 (Roh and Choi, 2016), was not able to mediate the TNF $\alpha$ -induced homo-dimerization and activation of MST1 (Figure S5E).

### MST1 Negatively Regulates TNF $\alpha$ -Induced NF- $\kappa$ B Signaling in Primary BMDMs

Finally, we investigated the possible role of MST1-mediated HOIP phosphorylation in the TNF $\alpha$ -induced activation of macrophages. First, we checked the importance of HOIP for TNF $\alpha$ -induced NF- $\kappa$ B signaling in primary mouse bone marrow-derived macrophages (BMDMs). BMDMs were transfected with control or HOIP siRNAs and then examined for TNF $\alpha$ -induced phosphorylation of I $\kappa$ B $\alpha$ . Whereas TNF $\alpha$  induced the phosphorylation of I $\kappa$ B $\alpha$  in BMDMs transfected with control siRNA, this effect was greatly attenuated in those depleted of HOIP (Figure S6A). Moreover, the siRNA-induced depletion of HOIP reduced the TNF $\alpha$ -induced production of IL-6 by BMDMs (Figure S6B). These results revealed that HOIP is required for activation of the NF- $\kappa$ B signaling pathway by TNF $\alpha$  in BMDMs. Consistent with the results from WT MEFs (Figure 6C), TNF $\alpha$  induced the interaction between HOIP and MST1 within TNF-RSC in WT BMDMs (Figure S6C). Additionally, immunoblot analysis with phospho-HOIP (Ser1066) antibody revealed that TNF $\alpha$  induced the phosphorylation of HOIP in WT BMDMs but not in MST1<sup>-/-</sup> BMDMs (Figure 7A), confirming the MST1-mediated phosphorylation of HOIP in TNF $\alpha$ -stimulated macrophages.

Next, we examined whether MST1 negatively regulates the TNF $\alpha$ -induced formation of linear Ub chains in BMDMs. TNF $\alpha$  increased total linear ubiquitination (Figure S6D) as well as the linear ubiquitination of NEMO (Figure 7B) in WT BMDMs, and these effects of TNF $\alpha$  were further enhanced in MST1<sup>-/-</sup> cells (Figures 7B and S6D). Given that the linear ubiquitination of NEMO by LUBAC promotes activation of the IKK complex (Tokunaga et al., 2009), we examined the levels of phosphorylated (activated) IKK $\alpha$ / $\beta$  complexed with NEMO in WT and MST1<sup>-/-</sup> BMDMs. Ablation of MST1 increased the amount of the phosphorylated (activated) IKK complex in TNF $\alpha$ -treated cells (Figure 7B). Additionally, MST1 deficiency also enhanced the effect of TNF $\alpha$  on the IKK-downstream signaling events including phosphorylation and degradation of I $\kappa$ B (Figure S6E) and phosphorylation (activation) of NF- $\kappa$ B p65 (Figure S6F) in BMDMs. Together, these results suggested that MST1



negatively regulates the LUBAC-mediated signaling events induced by TNF $\alpha$  in BMDMs.

To investigate the effect of HOIP phosphorylation on TNF $\alpha$ -induced linear ubiquitination in BMDMs, we transfected BMDMs with a *HOIP* siRNA to deplete endogenous HOIP and then reconstituted them with ectopic WT or S1066A mutant forms of human HOIP. The TNF $\alpha$ -induced formation of linear Ub chains was more pronounced in the cells expressing HOIP(S1066A) than in those expressing HOIP (Figure 7C). The extent of TNF $\alpha$ -induced IKK activation was also greater in the cells reconstituted with HOIP(S1066A) than in those reconstituted with HOIP (Figure 7C). Collectively, these results suggested that the MST1-mediated phosphorylation of HOIP negatively regulates the TNF $\alpha$ -induced formation of linear Ub chains and IKK activation in BMDMs.

Then, we examined the effect of MST1-mediated HOIP phosphorylation on the TNF $\alpha$ -induced expression of NF- $\kappa$ B target genes in BMDMs. WT and *MST1*<sup>-/-</sup> BMDMs depleted of endogenous HOIP were thus reconstituted with WT HOIP or HOIP(S1066A) and then assayed for the expression of NF- $\kappa$ B-regulated genes. TNF $\alpha$  increased the transcription of *IkB $\alpha$* , *IL-6*, and *iNOS* (Figure 7D), as well as the production of IL-6 protein and NO (Figure 7E) in the WT cells reconstituted with HOIP, and these effects of TNF $\alpha$  were enhanced further in those expressing HOIP(S1066A). Of note, genetic ablation of *MST1* in the cells reconstituted with WT HOIP enhanced the effects of TNF $\alpha$  on IL-6 and NO production to the levels observed in *MST1*<sup>-/-</sup> cells reconstituted with HOIP(S1066A). Together, these results suggested that MST1-mediated HOIP phosphorylation negatively regulates TNF $\alpha$ -induced NF- $\kappa$ B signaling in BMDMs.

## DISCUSSION

We have here uncovered a previously unrecognized function of MST1: namely, the negative regulation of TNF $\alpha$ -induced NF- $\kappa$ B signaling through phosphorylation of HOIP, the catalytic component of LUBAC. MST1 mediates the phosphorylation of human HOIP at Ser<sup>1,066</sup> and thereby inhibits the linear Ub chain-forming activity of LUBAC. It thus functions as a negative modulator of LUBAC-dependent NF- $\kappa$ B signaling events induced by TNF $\alpha$ .

The E3 ligase LUBAC plays an essential role in the NF- $\kappa$ B signaling pathway activated by TNF $\alpha$ . Now, we show that in response to TNF $\alpha$  stimulation, MST1 physically associates with HOIP, mediates its phosphorylation on Ser<sup>1,066</sup>, and thereby inhibits its linear Ub chain-forming activity. In resting cells, the LUBAC complex resides in the cytosol. In response to TNF $\alpha$  stimulation, however, the LUBAC components HOIP, HOIL-1L, and Sharpin are recruited to TNF-RSC, which forms immediately after the binding of TNF $\alpha$  to TNFR1 (Walczak et al., 2012). Importantly, we found that TNF $\alpha$  triggers the recruitment of MST1 to the TNF-RSC as well as the MST1 activation and MST1-HOIP interaction within the TNF-RSC complex. Thus, TNF $\alpha$  appears to induce the recruitment of both MST1 and HOIP to TNF-RSC, after which MST1 interacts with HOIP and mediates its phosphorylation on Ser<sup>1,066</sup>.

The Ser<sup>1,066</sup> residue is located in the LDD of HOIP, which serves as the binding site for the acceptor Ub molecule (Smit et al., 2012). The LDD domain is thus required for HOIP

to conjugate the COOH-terminus of the donor Ub to the NH<sub>2</sub>-terminus of the acceptor Ub (Smit et al., 2012). Given that LDD is essential for the catalytic activity of HOIP (Lechtenberg et al., 2016; Smit et al., 2012; Smit and Sixma, 2014; Stieglitz et al., 2013), we propose that Ser<sup>1,066</sup> phosphorylation may be the primary mechanism by which MST1 inhibits the E3 ligase activity of HOIP. Indeed, MST1 suppresses the E3 activity of HOIP but not that of the HOIP(S1066A) mutant. With regard to the mechanism by which S<sup>1,066</sup>-phosphorylation interferes with the E3 ligase activity of HOIP, our *in vitro* binding data indicate that MST1-mediated Ser<sup>1,066</sup> phosphorylation inhibits the interaction of HOIP(LDD) with linear Ub chains. Whereas the phosphorylation-defective S1066A mutant of HOIP(LDD) was resistant to the inhibitory action of MST1 on binding to linear Ub chains, the phosphomimetic mutants S1066D and S1066E were defective in the ability to bind to linear Ub chains. Together, these data suggest that MST1-mediated phosphorylation of HOIP at Ser<sup>1,066</sup> suppresses Ub recognition by LDD of HOIP and thereby inhibits the linear Ub chain-forming E3 activity of this protein.

The scaffold protein TRAF2 plays an essential role in the TNF $\alpha$ -induced formation of TNF-RSC (Wajant and Scheurich, 2001). In this study, we found that TNF $\alpha$  induces the interaction of MST1 with TRAF2, and that TRAF2 mediates the TNF $\alpha$ -induced recruitment of MST1 to TNF-RSC and MST1 activation. These findings suggest that TNF $\alpha$  induces the recruitment of both MST1 and TRAF2 to TNF-RSC, and TRAF2 consequently binds and activates MST1 as well as promotes the MST1-HOIP interaction and MST1-mediated HOIP phosphorylation within the TNF-RSC complex. Of note, we have observed that TWEAK and CD40L, both of which belong to the TNF superfamily ligands that promote activation of the NF- $\kappa$ B signaling (Bodmer et al., 2002), induce the activation of MST1 (Figure S7A) but do not promote the MST1-dependent phosphorylation of HOIP in MEFs (Figure S7B). MST1 deficiency also does not affect the TWEAK- or CD40L-induced formation of linear Ub-chains and IKK phosphorylation (activation) in MEFs (Figure S7A). At present, it is unclear why MST1-mediated HOIP phosphorylation takes place after TNF $\alpha$  stimulation but not after TWEAK or CD40L stimulation, raising the mechanistic question about a role of TRAF2 in the activation of MST1 induced by each of these stimuli.

NF- $\kappa$ B is a master transcription factor that plays a pivotal role in immune responses. Strict regulation of the NF- $\kappa$ B signaling pathway is thus critical for maintenance of immune homeostasis. Uncontrolled overactivation of this pathway may result in excessive inflammation that can eventually give rise to various pathological conditions. Thus, it is important that the initiation and propagation of NF- $\kappa$ B signaling be countered by negative regulatory mechanisms that attenuate extensive signaling activity and thereby promote the resolution of inflammation and prevent unwanted tissue damage. Studies of such negative regulation of NF- $\kappa$ B signaling have mostly focused on the reversal of ubiquitination mediated by deubiquitinases such as CYLD, OTULIN, and A20 (Keusekotten et al., 2013; Kovalenko et al., 2003; Lafont et al., 2018; Song et al., 1996; Trompouki et al., 2003). Our findings reveal a previously unrecognized mechanism for negative regulation of the NF- $\kappa$ B pathway, in which MST1 attenuates NF- $\kappa$ B-dependent inflammatory gene expression by phosphory-

lating HOIP. Our identification of MST1-mediated inhibition of HOIP activity thus extends understanding of negative regulation of the NF- $\kappa$ B pathway and thereby provides better insight into the control of immune homeostasis.

## STAR★METHODS

Detailed methods are provided in the online version of this paper and include the following:

- KEY RESOURCES TABLE
- CONTACT FOR REAGENT AND RESOURCE SHARING
- EXPERIMENTAL MODEL AND SUBJECT DETAILS
  - Cell culture and DNA transfection
  - Plasmids, antibodies, and reagents
  - Co-immunoprecipitation and immunoblot analysis
  - Quantitative RT-PCR analysis
  - Mass Spectrometry of phosphoproteins
  - Immune complex kinase assay
  - *In vitro* binding assays
  - *In vitro* ubiquitination assays
  - Pull-down assay of linear ubiquitin chains using GST-fused M1-SUB
  - Immunofluorescence analysis
  - *In situ* PLA
  - RNAi
  - Analysis of TNF-RSC
  - pIMAGO-based detection of phosphorylated proteins
  - Nuclear fractionation and NF- $\kappa$ B p65 ELISA
  - IL-6 ELISA
  - Administration of TNF $\alpha$
  - Statistical analysis
- DATA AND SOFTWARE AVAILABILITY

## SUPPLEMENTAL INFORMATION

Supplemental Information includes seven figures and can be found with this article online at <https://doi.org/10.1016/j.molcel.2019.01.022>.

## ACKNOWLEDGMENTS

We thank K. Iwai for GST-hTNF $\alpha$ (77–233) cDNA, S. Yonehara for Flag-MST1 cDNA, V.M. Dixit for antibody to linear ubiquitin, S.Y. Lee for TRAF2<sup>+/+</sup> or TRAF2<sup>-/-</sup> MEFs, and D.S. Lim for MST1<sup>-/-</sup> mice. This work was supported by a National Research Foundation grant (NRF-2017R1A2B2008193) and by a BRL grant (NRF-2015R1A4A1041919) funded by the Ministry of Science and ICT of Korea as well as by a Korea University grant (E.-J.C.).

## AUTHOR CONTRIBUTIONS

I.Y.L., J.M.L., H.C., E.K., Y.K., H.K.O., W.S.Y., K.H.R., and J.-H.Y. conducted the experiments; I.Y.L., J.-H.Y., H.W.P., J.-S.M., H.K.S., and E.-J.C. designed the experiments; and I.Y.L. and E.-J.C. wrote the paper.

## DECLARATION OF INTERESTS

The authors declare no competing interests.

Received: May 9, 2018

Revised: November 20, 2018

Accepted: January 14, 2019

Published: February 14, 2019

## REFERENCES

- Berger, S.B., Kasparcova, V., Hoffman, S., Swift, B., Dare, L., Schaeffer, M., Capriotti, C., Cook, M., Finger, J., Hughes-Earle, A., et al. (2014). Cutting Edge: RIP1 kinase activity is dispensable for normal development but is a key regulator of inflammation in SHARPIN-deficient mice. *J. Immunol.* **192**, 5476–5480.
- Bertrand, M.J., Milutinovic, S., Dickson, K.M., Ho, W.C., Boudreau, A., Durkin, J., Gillard, J.W., Jaquith, J.B., Morris, S.J., and Barker, P.A. (2008). cIAP1 and cIAP2 facilitate cancer cell survival by functioning as E3 ligases that promote RIP1 ubiquitination. *Mol. Cell* **30**, 689–700.
- Bodmer, J.L., Schneider, P., and Tschopp, J. (2002). The molecular architecture of the TNF superfamily. *Trends Biochem. Sci.* **27**, 19–26.
- Chae, J.S., Gil Hwang, S., Lim, D.S., and Choi, E.J. (2012). Thioredoxin-1 functions as a molecular switch regulating the oxidative stress-induced activation of MST1. *Free Radic. Biol. Med.* **53**, 2335–2343.
- Chen, Z.J. (2012). Ubiquitination in signaling to and activation of IKK. *Immunol. Rev.* **246**, 95–106.
- Cheung, W.L., Ajiro, K., Samejima, K., Kloc, M., Cheung, P., Mizzen, C.A., Beeser, A., Etkin, L.D., Chernoff, J., Earnshaw, W.C., and Allis, C.D. (2003). Apoptotic phosphorylation of histone H2B is mediated by mammalian sterile twenty kinase. *Cell* **113**, 507–517.
- Cho, S.G., Kim, J.W., Lee, Y.H., Hwang, H.S., Kim, M.S., Ryoo, K., Kim, M.J., Noh, K.T., Kim, E.K., Cho, J.H., et al. (2003). Identification of a novel antiapoptotic protein that antagonizes ASK1 and CAD activities. *J. Cell Biol.* **163**, 71–81.
- Creasy, C.L., and Chernoff, J. (1995). Cloning and characterization of a member of the MST subfamily of Ste20-like kinases. *Gene* **167**, 303–306.
- Creasy, C.L., Ambrose, D.M., and Chernoff, J. (1996). The Ste20-like protein kinase, Mst1, dimerizes and contains an inhibitory domain. *J. Biol. Chem.* **271**, 21049–21053.
- Damgaard, R.B., Nachbur, U., Yabal, M., Wong, W.W., Fiil, B.K., Kastir, M., Rieser, E., Rickard, J.A., Bankovacki, A., Peschel, C., et al. (2012). The ubiquitin ligase XIAP recruits LUBAC for NOD2 signaling in inflammation and innate immunity. *Mol. Cell* **46**, 746–758.
- Ea, C.K., Deng, L., Xia, Z.P., Pineda, G., and Chen, Z.J. (2006). Activation of IKK by TNF $\alpha$  requires site-specific ubiquitination of RIP1 and polyubiquitin binding by NEMO. *Mol. Cell* **22**, 245–257.
- Gerlach, B., Cordier, S.M., Schmukle, A.C., Emmerich, C.H., Rieser, E., Haas, T.L., Webb, A.I., Rickard, J.A., Anderton, H., Wong, W.W., et al. (2011). Linear ubiquitination prevents inflammation and regulates immune signalling. *Nature* **471**, 591–596.
- Haas, T.L., Emmerich, C.H., Gerlach, B., Schmukle, A.C., Cordier, S.M., Rieser, E., Feltham, R., Vince, J., Warnken, U., Wenger, T., et al. (2009). Recruitment of the linear ubiquitin chain assembly complex stabilizes the TNF-R1 signaling complex and is required for TNF-mediated gene induction. *Mol. Cell* **36**, 831–844.
- Hostager, B.S., Fox, D.K., Whitten, D., Wilkerson, C.G., Eipper, B.A., Francone, V.P., Rothman, P.B., and Colgan, J.D. (2010). HOIL-1L interacting protein (HOIP) as an NF- $\kappa$ B regulating component of the CD40 signaling complex. *PLoS ONE* **5**, e11380.
- Hostager, B.S., Kashiwada, M., Colgan, J.D., and Rothman, P.B. (2011). HOIL-1L interacting protein (HOIP) is essential for CD40 signaling. *PLoS ONE* **6**, e23061.
- Hsu, H., Shu, H.B., Pan, M.G., and Goeddel, D.V. (1996). TRADD-TRAF2 and TRADD-FADD interactions define two distinct TNF receptor 1 signal transduction pathways. *Cell* **84**, 299–308.
- Ikeda, F., Deribe, Y.L., Skånland, S.S., Stieglitz, B., Grabbe, C., Franz-Wachtel, M., van Wijk, S.J., Goswami, P., Nagy, V., Terzic, J., et al. (2011). SHARPIN forms a linear ubiquitin ligase complex regulating NF- $\kappa$ B activity and apoptosis. *Nature* **471**, 637–641.
- Inn, K.S., Gack, M.U., Tokunaga, F., Shi, M., Wong, L.Y., Iwai, K., and Jung, J.U. (2011). Linear ubiquitin assembly complex negatively regulates RIG-I and TRIM25-mediated type I interferon induction. *Mol. Cell* **41**, 354–365.
- Keusekotten, K., Elliott, P.R., Glockner, L., Fiil, B.K., Damgaard, R.B., Kulathu, Y., Wauer, T., Hospenthal, M.K., Gyrd-Hansen, M., Krappmann, D., et al. (2013). OTULIN antagonizes LUBAC signaling by specifically hydrolyzing Met1-linked polyubiquitin. *Cell* **153**, 1312–1326.
- Kirisako, T., Kamei, K., Murata, S., Kato, M., Fukumoto, H., Kanie, M., Sano, S., Tokunaga, F., Tanaka, K., and Iwai, K. (2006). A ubiquitin ligase complex assembles linear polyubiquitin chains. *EMBO J.* **25**, 4877–4887.
- Kovalenko, A., Chable-Bessia, C., Cantarella, G., Israël, A., Wallach, D., and Courtois, G. (2003). The tumour suppressor CYLD negatively regulates NF- $\kappa$ B signalling by deubiquitination. *Nature* **424**, 801–805.
- Lafont, E., Hartwig, T., and Walczak, H. (2018). Paving TRAIL's path with ubiquitin. *Trends Biochem. Sci.* **43**, 44–60.
- Lechtenberg, B.C., Rajput, A., Sanishvili, R., Dobaczewska, M.K., Ware, C.F., Mace, P.D., and Riedl, S.J. (2016). Structure of a HOIP/E2~ubiquitin complex reveals RBR E3 ligase mechanism and regulation. *Nature* **529**, 546–550.
- Lehtinen, M.K., Yuan, Z., Boag, P.R., Yang, Y., Villén, J., Becker, E.B., DiBacco, S., de la Iglesia, N., Gygi, S., Blackwell, T.K., and Bonni, A. (2006). A conserved MST-FOXO signaling pathway mediates oxidative-stress responses and extends life span. *Cell* **125**, 987–1001.
- Meng, Z., Moroishi, T., Mottier-Pavie, V., Plouffe, S.W., Hansen, C.G., Hong, A.W., Park, H.W., Mo, J.S., Lu, W., Lu, S., et al. (2015). MAP4K family kinases act in parallel to MST1/2 to activate LATS1/2 in the Hippo pathway. *Nat. Commun.* **6**, 8357.
- Micheau, O., and Tschopp, J. (2003). Induction of TNF receptor I-mediated apoptosis via two sequential signaling complexes. *Cell* **114**, 181–190.
- Oh, H.J., Lee, K.K., Song, S.J., Jin, M.S., Song, M.S., Lee, J.H., Im, C.R., Lee, J.O., Yonehara, S., and Lim, D.S. (2006). Role of the tumor suppressor RASSF1A in Mst1-mediated apoptosis. *Cancer Res.* **66**, 2562–2569.
- Ohtsubo, H., Ichiki, T., Imayama, I., Ono, H., Fukuyama, K., Hashiguchi, Y., Sadoshima, J., and Sunagawa, K. (2008). Involvement of Mst1 in tumor necrosis factor- $\alpha$ -induced apoptosis of endothelial cells. *Biochem. Biophys. Res. Commun.* **367**, 474–480.
- Park, H.S., Lee, J.S., Huh, S.H., Seo, J.S., and Choi, E.J. (2001). Hsp72 functions as a natural inhibitory protein of c-Jun N-terminal kinase. *EMBO J.* **20**, 446–456.
- Park, J., Kang, S.I., Lee, S.Y., Zhang, X.F., Kim, M.S., Beers, L.F., Lim, D.S., Avruch, J., Kim, H.S., and Lee, S.B. (2010). Tumor suppressor ras association domain family 5 (RASSF5/NORE1) mediates death receptor ligand-induced apoptosis. *J. Biol. Chem.* **285**, 35029–35038.
- Peltzer, N., Rieser, E., Taraborrelli, L., Draber, P., Darding, M., Pernaute, B., Shimizu, Y., Sarr, A., Draberova, H., Montinaro, A., et al. (2014). HOIP deficiency causes embryonic lethality by aberrant TNFR1-mediated endothelial cell death. *Cell Rep.* **9**, 153–165.
- Pickart, C.M. (2001). Mechanisms underlying ubiquitination. *Annu. Rev. Biochem.* **70**, 503–533.
- Radu, M., and Chernoff, J. (2009). The DeMSTification of mammalian Ste20 kinases. *Curr. Biol.* **19**, R421–R425.
- Rahighi, S., Ikeda, F., Kawasaki, M., Akutsu, M., Suzuki, N., Kato, R., Kensche, T., Uejima, T., Bloor, S., Komander, D., et al. (2009). Specific recognition of linear ubiquitin chains by NEMO is important for NF- $\kappa$ B activation. *Cell* **136**, 1098–1109.
- Rawat, S.J., and Chernoff, J. (2015). Regulation of mammalian Ste20 (Mst) kinases. *Trends Biochem. Sci.* **40**, 149–156.
- Rickard, J.A., Anderton, H., Etemudi, N., Nachbur, U., Darding, M., Peltzer, N., Lalaoui, N., Lawlor, K.E., Vanyai, H., Hall, C., et al. (2014). TNFR1-dependent cell death drives inflammation in Sharpin-deficient mice. *eLife* **3**, 3.
- Roh, K.H., and Choi, E.J. (2016). TRAF2 functions as an activator switch in the reactive oxygen species-induced stimulation of MST1. *Free Radic. Biol. Med.* **91**, 105–113.
- Ryoo, K., Huh, S.H., Lee, Y.H., Yoon, K.W., Cho, S.G., and Choi, E.J. (2004). Negative regulation of MEKK1-induced signaling by glutathione S-transferase Mu. *J. Biol. Chem.* **279**, 43589–43594.

- Scheel, H., and Hofmann, K. (2003). A novel interaction motif, SARAH, connects three classes of tumor suppressor. *Curr. Biol.* *13*, R899–R900.
- Shu, H.B., Takeuchi, M., and Goeddel, D.V. (1996). The tumor necrosis factor receptor 2 signal transducers TRAF2 and c-IAP1 are components of the tumor necrosis factor receptor 1 signaling complex. *Proc. Natl. Acad. Sci. USA* *93*, 13973–13978.
- Smit, J.J., and Sixma, T.K. (2014). RBR E3-ligases at work. *EMBO Rep.* *15*, 142–154.
- Smit, J.J., Monteferrario, D., Noordermeer, S.M., van Dijk, W.J., van der Reijden, B.A., and Sixma, T.K. (2012). The E3 ligase HOIP specifies linear ubiquitin chain assembly through its RING-IBR-RING domain and the unique LDD extension. *EMBO J.* *31*, 3833–3844.
- Song, H.Y., Rothe, M., and Goeddel, D.V. (1996). The tumor necrosis factor-inducible zinc finger protein A20 interacts with TRAF1/TRAF2 and inhibits NF- $\kappa$ B activation. *Proc. Natl. Acad. Sci. USA* *93*, 6721–6725.
- Stieglitz, B., Rana, R.R., Koliopoulos, M.G., Morris-Davies, A.C., Schaeffer, V., Christodoulou, E., Howell, S., Brown, N.R., Dikic, I., and Rittinger, K. (2013). Structural basis for ligase-specific conjugation of linear ubiquitin chains by HOIP. *Nature* *503*, 422–426.
- Tokunaga, F., and Iwai, K. (2012). Linear ubiquitination: a novel NF- $\kappa$ B regulatory mechanism for inflammatory and immune responses by the LUBAC ubiquitin ligase complex. *Endocr. J.* *59*, 641–652.
- Tokunaga, F., Sakata, S., Saeki, Y., Satomi, Y., Kirisako, T., Kamei, K., Nakagawa, T., Kato, M., Murata, S., Yamaoka, S., et al. (2009). Involvement of linear polyubiquitylation of NEMO in NF- $\kappa$ B activation. *Nat. Cell Biol.* *11*, 123–132.
- Tokunaga, F., Nakagawa, T., Nakahara, M., Saeki, Y., Taniguchi, M., Sakata, S., Tanaka, K., Nakano, H., and Iwai, K. (2011). SHARPIN is a component of the NF- $\kappa$ B-activating linear ubiquitin chain assembly complex. *Nature* *471*, 633–636.
- Trompouki, E., Hatzivassiliou, E., Tschirritzis, T., Farmer, H., Ashworth, A., and Mosialos, G. (2003). CYLD is a deubiquitinating enzyme that negatively regulates NF- $\kappa$ B activation by TNFR family members. *Nature* *424*, 793–796.
- Vallabhapurapu, S., and Karin, M. (2009). Regulation and function of NF- $\kappa$ B transcription factors in the immune system. *Annu. Rev. Immunol.* *27*, 693–733.
- Varfolomeev, E., Goncharov, T., Maecker, H., Zobel, K., Kömüves, L.G., Deshayes, K., and Vucic, D. (2012). Cellular inhibitors of apoptosis are global regulators of NF- $\kappa$ B and MAPK activation by members of the TNF family of receptors. *Sci. Signal.* *5*, ra22.
- Wajant, H., and Scheurich, P. (2001). Tumor necrosis factor receptor-associated factor (TRAF) 2 and its role in TNF signaling. *Int. J. Biochem. Cell Biol.* *33*, 19–32.
- Walczak, H., Iwai, K., and Dikic, I. (2012). Generation and physiological roles of linear ubiquitin chains. *BMC Biol.* *10*, 23.
- Wepf, A., Glatter, T., Schmidt, A., Aebersold, R., and Gstaiger, M. (2009). Quantitative interaction proteomics using mass spectrometry. *Nat. Methods* *6*, 203–205.
- Yuan, Z., Lehtinen, M.K., Merlo, P., Villén, J., Gygi, S., and Bonni, A. (2009). Regulation of neuronal cell death by MST1-FOXO1 signaling. *J. Biol. Chem.* *284*, 11285–11292.
- Yun, H.J., Yoon, J.H., Lee, J.K., Noh, K.T., Yoon, K.W., Oh, S.P., Oh, H.J., Chae, J.S., Hwang, S.G., Kim, E.H., et al. (2011). Daxx mediates activation-induced cell death in microglia by triggering MST1 signalling. *EMBO J.* *30*, 2465–2476.
- Zak, D.E., Schmitz, F., Gold, E.S., Diercks, A.H., Peschon, J.J., Valvo, J.S., Niemistö, A., Podolsky, I., Fallen, S.G., Suen, R., et al. (2011). Systems analysis identifies an essential role for SHANK-associated RH domain-interacting protein (SHARPIN) in macrophage Toll-like receptor 2 (TLR2) responses. *Proc. Natl. Acad. Sci. USA* *108*, 11536–11541.
- Zhang, M., Tian, Y., Wang, R.P., Gao, D., Zhang, Y., Diao, F.C., Chen, D.Y., Zhai, Z.H., and Shu, H.B. (2008). Negative feedback regulation of cellular antiviral signaling by RBCK1-mediated degradation of IRF3. *Cell Res.* *18*, 1096–1104.

## STAR★METHODS

### KEY RESOURCES TABLE

REAGENT or RESOURCE	SOURCE	IDENTIFIER
<b>Antibodies</b>		
Rabbit polyclonal anti-MST1	Cell Signaling Technology	Cat#3682; RRID: AB_2144632
Rabbit polyclonal anti-MST2	Cell Signaling Technology	Cat#3952; RRID: AB_2196471
Rabbit polyclonal anti-phospho-MST1(Thr183)/MST2(Thr180)	Cell Signaling Technology	Cat#3681; RRID: AB_330269
Rabbit polyclonal anti-I $\kappa$ B- $\alpha$	Cell Signaling Technology	Cat#9242; RRID: AB_823540
Rabbit monoclonal anti-Phospho-NF- $\kappa$ B p65 (Ser536) (93H1)	Cell Signaling Technology	Cat#3033; RRID: AB_331284
Mouse monoclonal anti-Phospho-I $\kappa$ B $\alpha$ (Ser32/36)	Cell Signaling Technology	Cat#9246; RRID: AB_2267145
Rabbit monoclonal anti-Phospho-IKK $\alpha$ / $\beta$ (Ser176/180)	Cell Signaling Technology	Cat#2697; RRID: AB_2079382
Rabbit monoclonal anti-CYLD (D1A10)	Cell Signaling Technology	Cat#8462; RRID: AB_10949157
Rabbit monoclonal anti-A20/TNFAIP3 (D13H3)	Cell Signaling Technology	Cat#5630; RRID: AB_10698880
Rabbit polyclonal anti-NF- $\kappa$ B p65	Santa Cruz Biotechnology	Cat#sc-109; RRID: AB_632039
Rabbit polyclonal anti-IKK $\gamma$ (FL-419)	Santa Cruz Biotechnology	Cat#sc-8330; RRID: AB_2124846
Rabbit polyclonal anti-IKK $\alpha$ / $\beta$ (H-470)	Santa Cruz Biotechnology	Cat#sc-7607; RRID: AB_675667
Rabbit polyclonal anti-His <sub>6</sub> -probe (H-15)	Santa Cruz Biotechnology	Cat#sc-803; RRID: AB_631655
Rabbit polyclonal anti-TRAF2 (C-20)	Santa Cruz Biotechnology	Cat#sc-876; RRID: AB_632533
Mouse monoclonal anti-TNF-R1 (H-5)	Santa Cruz Biotechnology	Cat#sc-8436; RRID: AB_628377
Mouse monoclonal anti-RIP (clone 38)	BD Biosciences	Cat#610458; RRID: AB_397831
Mouse monoclonal anti-Flag (clone M2)	Sigma-Aldrich	Cat#F1804; RRID: AB_262044
Mouse monoclonal anti-IKK $\gamma$ (clone EA2-6)	MBL International	Cat#K0159-3; RRID: AB_591987
Rabbit polyclonal anti-RNF31/HOIP	Abcam	Cat#ab85294; RRID: AB_1925400
Rabbit polyclonal anti-RBCK1/HOIL-1L	Abcam	Cat#ab38540; RRID: AB_777638
Mouse monoclonal anti-Maltose Binding Protein [MBP-17] (HRP)	Abcam	Cat#ab49923; RRID: AB_881602
Goat polyclonal anti-mouse TNF-alpha	R&D Systems	Cat#AF-410-NA; RRID: AB_354479
Rabbit monoclonal anti-ubiquitin, Lys63-specific (clone Apu3)	Millipore	Cat#05-1308; RRID: AB_1587580
Rabbit polyclonal anti-Sharpin	Proteintech Group	Cat#14626-1-AP; RRID: AB_2187734
Anti-Linear Polyubiquitin	Genentech	N/A
Rabbit polyclonal anti-HA-probe (Y-11)	Santa Cruz Biotechnology	Cat#sc-805; RRID: AB_631618
Rabbit polyclonal anti-c-Myc (A-14)	Santa Cruz Biotechnology	Cat#sc-789; RRID: AB_631274
Rabbit polyclonal anti-GST (Z-5)	Santa Cruz Biotechnology	Cat#sc-459; RRID: AB_631586
Mouse monoclonal anti-GAPDH (6C5)	Santa Cruz Biotechnology	Cat#sc-32233; RRID: AB_627679
Mouse monoclonal anti-Ub (P4D1)	Santa Cruz Biotechnology	Cat#sc-8017; RRID: AB_628423
Rabbit polyclonal anti-c-IAP1	Cell Signaling Technology	Cat#4952; RRID: AB_2063660
Rabbit polyclonal anti-phospho-HOIP (Ser1066)	This paper	N/A
<b>Bacterial and Virus Strains</b>		
<i>E. coli</i> : BL21 star (DE3) competent cells	Invitrogen	C601003
<b>Chemicals, Peptides, and Recombinant Proteins</b>		
Recombinant Murine TNF- $\alpha$	Peptotech	315-01A
Recombinant Murine sCD40 Ligand	Peptotech	315-15
Recombinant Mouse sWEAK/TNFSF12 Protein	R&D Systems	1237-TW
Staurosporine from <i>Streptomyces</i> sp.	Sigma-Aldrich	S5921; CAS 62996-74-1
ATP, [ $\gamma$ - <sup>32</sup> P]-3000Ci/mmol	Perkin Elmer	BLU002A250UC
EasyTag L-[ <sup>35</sup> S]-Methionine	Perkin Elmer	NEG709A500UC
Griess reagent (modified)	Sigma-Aldrich	G4410
TRIZOL Reagent	Invitrogen	15596-026

(Continued on next page)

**Continued**

REAGENT or RESOURCE	SOURCE	IDENTIFIER
MMLV Reverse Transcriptase	Beams Biotechnology	3201
Maxima SYBR Green/Fluorescein qPCR Master Mix (2X)	Thermo Fisher Scientific	K0241
Protein G Sepharose 4 Fast Flow	GE Healthcare	17-0618-02
Ni-NTA Chelating Agarose CL-6B	Incospharm	1103-2
Glutathione Agarose 4B	Incospharm	1101-2
His <sub>6</sub> -Ubiquitin E1 enzyme (UBE1)	BostonBiochem	E-304
UbcH5c Conjugating Enzyme	Millipore	14-811
Ubiquitin from bovine erythrocytes	Sigma-Aldrich	U6253; CAS 79586-22-4
Adenosine 5'-triphosphate disodium salt hydrate	Sigma-Aldrich	A6419; CAS 34369-07-8
Ubiquitin from bovine erythrocytes	Sigma-Aldrich	U6253; CAS 79586-22-4
MST1, active	Millipore	14-624
Recombinant human RNF31/HOIP protein (Catalytic domain)	Abcam	Ab189235
GST control	This paper	N/A
GST-tagged HOIP (1-480, 481-632, 633-1072, 633-909, or 910-1072) proteins	This paper	N/A
His <sub>6</sub> -tagged MST1 protein	This paper	N/A
GST-tagged NEMO (257-346) protein, M1-SUB	This paper	N/A
GST-tagged hTNF $\alpha$ (77-233) protein	This paper	N/A
MBP control	This paper	N/A
MBP-tagged HOIP [910-1072 (WT, S1066A, S1066D, or S1066E)] proteins	This paper	N/A
GST-linear Ub4	This paper	N/A
<b>Biological Samples</b>		
Mouse lung tissue	This paper	N/A
<b>Critical Commercial Assays</b>		
Duolink <i>In Situ</i> Detection Reagents Red	Sigma-Aldrich	DUO92008
pMAGO-biotin Phosphoprotein Detection Kit for Western Blot	Tymora Analytical Operations	800-40
TransAM NF $\kappa$ B p65	Active Motif	40096
Mouse IL-6 Platinum ELISA Kit	Invitrogen	BMS603-2
TNT Quick Coupled Transcription/Translation Systems	Promega	L1170
<b>Deposited Data</b>		
Raw data	This paper; Mendeley Data	<a href="http://doi.org/10.17632/d5k5jv8ygt.1">http://doi.org/10.17632/d5k5jv8ygt.1</a>
<b>Experimental Models: Cell Lines</b>		
HEK293T	N/A	N/A
Wild-type MEF	This paper	N/A
MST1 knockout MEF	This paper	N/A
TRAF2 knockout MEF	Gift from S.Y. Lee	N/A
HEK293A WT and MST1/2 dKO	<a href="#">Meng et al., 2015.</a>	N/A
Primary BMDMs WT and MST1 <sup>-/-</sup>	This paper	N/A
<b>Experimental Models: Organisms/Strains</b>		
Mouse: C57BL/6 MST1 <sup>-/-</sup>	Gift from D.S. Lim	N/A
<b>Oligonucleotides</b>		
siRNA sequence for mHOIP #1, 5'-GAGGACGGAGUUGUGAGGAUUUCCA-3'	This paper	N/A
siRNA sequence for mHOIP #2, 5'-CUGCUAAGAGAGAGCGUUGAAGAUG-3'	This paper	N/A
siRNA sequence for scrambled control, 5'-GAGGGCUGAUGAGUAGUUGACCA-3'	This paper	N/A

(Continued on next page)

**Continued**

REAGENT or RESOURCE	SOURCE	IDENTIFIER
siRNA sequence for mMST2, 5'-CCCAUGAUGGAACGAGAAUA-3'	This paper	N/A
siRNA sequence for scrambled control, 5'-CGUACGCGAAUACUUCGAUU-3'	This paper	N/A
Primer sequence for I $\kappa$ B $\alpha$ , Forward: 5'-CGCTTGGTGGACGATCG-3' Reverse: 5'-TTGCTCGTACTCCTCGTCCTTC-3'	This paper	N/A
Primer sequence for IL-6, Forward: 5' TCTAATTCATATCTTCAACCAAGAGG-3' Reverse: 5'-TGGTCCTTAGCCACTCCTTC-3'	This paper	N/A
Primer sequence for iNOS, Forward: 5'-CTTTGCCACGGACGAGAC Reverse: 5'-TCATTGTACTCTGAGGGCTGAC-3'	This paper	N/A
Primer sequence for GAPDH, Forward: 5'-CGTGCCGCTGGAGAAACC-3' Reverse: 5'-CTTACCACCTTCTTGATGTC-3'	This paper	N/A
<b>Recombinant DNA</b>		
Flag-HOIP expressing plasmid	GeneCopoeia	EX-Z1067-M14
HA-Sharpin expressing plasmid	GeneCopoeia	EX-T7922-M07
Myc-HOIL-1L expressing plasmid	GeneCopoeia	EX-E2001-M09
HA-OTULIN expressing plasmid	GeneCopoeia	EX-H2249-M06
HA-CYLD expressing plasmid	Addgene	15506
Flag-HOIP (S1066A or S1066E) expressing plasmid	This paper	N/A
Flag-MST1 expressing plasmid	Gift from S. Yonehara	N/A
Flag-MST1 (K59R) expressing plasmid	This paper	N/A
Myc-MST1 (Full-length, 1-326, or 327-487) expressing plasmid	This paper	N/A
HA-MST1 (WT, or K59R) expressing plasmid	This paper	N/A
HA-TRAF2 (Full-length or 272-501) expressing plasmid	This paper	N/A
GST-tagged hTNF $\alpha$ (77-233) expressing plasmid	Gift from K. Iwai	N/A
GST-tagged HOIP (1-480, 481-632, 633-1072, 633-909, or 910-1072) expressing plasmid	This paper	N/A
Flag-MST2 expressing plasmid	Gift from D.S. Lim	N/A
GST-tagged NEMO (257-233) expressing plasmid	This paper	N/A
His <sub>6</sub> -tagged MST1 (K59R) expressing plasmid	This paper	N/A
<b>Software and Algorithms</b>		
Photoshop CC 2015	Adobe Software	RRID: SCR_014199
ImageJ	ImageJ Software	RRID: SCR_003070
Zen 2 (blue edition)	Carl-Zeiss software	RRID: SCR_013672

**CONTACT FOR REAGENT AND RESOURCE SHARING**

Further information and requests for reagents may be directed to and will be fulfilled by the Lead Contact, Eui-Ju Choi ([ejchoi@korea.ac.kr](mailto:ejchoi@korea.ac.kr)).

**EXPERIMENTAL MODEL AND SUBJECT DETAILS**

**Cell culture and DNA transfection**

For primary culture of BMDMs, bone marrow cells were isolated from the hind leg bones of WT or MST1<sup>-/-</sup> C57BL/6 mice, which were described previously (Oh et al., 2006). The cells were plated in 100-mm culture dishes (5 × 10<sup>6</sup> cells/dish) and maintained in DMEM supplemented with recombinant murine M-CSF (40 ng/mL, Peprotech). After 7 days, nonadherent cells were removed and adherent cells were harvested for experiments. All animal procedures were approved by the Institutional Animal Care and Use Committee of Korea University. WT and MST1<sup>-/-</sup> MEFs were prepared from WT and MST1<sup>-/-</sup> mice, respectively, as described

previously (Chae et al., 2012). MEFs as well as HEK293 and MST1/2-dKO HEK293A cells (Meng et al., 2015) were cultured under a humidified atmosphere of 5% CO<sub>2</sub> at 37°C in DMEM supplemented with 10% FBS. For DNA transfection, indicated expression vectors were introduced into the cells with the use of either polyethylenimine (Sigma, St Louis, MO) for MEFs and HEK293 cells or the JetPEI reagent (Polyplus-transfection) for BMDMs.

### Plasmids, antibodies, and reagents

The plasmids pEZ-M14/Flag-HOIP, pEZ-M07/HA-SHARPIN, pReceiver-M09/Myc-HOIL-1L, and pEZ-M06/HA-OTULIN were obtained from GeneCopoeia (Rockville, MD) and pDEST-HA/HA-CYLD was from Addgene (Cambridge, MA). All of these vectors were for human proteins. The Flag-HOIP (S1066A and S1066E) mutant constructs were prepared by site-directed mutagenesis with pEZ-M14/Flag-HOIP as template. The plasmid pME18S/Flag-MST1 was kindly provided by S. Yonehara (Kyoto University, Japan) and the Flag-MST1(K59R) mutant construct was generated by site-directed mutagenesis with pME18S/Flag-MST1 as template. pET23b/His<sub>6</sub>-MST1(K59R), pHM6/HA-MST1(WT or K59R), and pcDNA3/Myc-MST1 were described previously (Chae et al., 2012; Oh et al., 2006; Yun et al., 2011). cDNA of MST1[(1-326) or (327-487)] in pcCMV5a/Flag-MST1[(1-326) or (327-487)] was subcloned into pcDNA6/Myc-His B to generate pcDNA6/Myc-His B-MST1[(1-326) or (327-487)], respectively. For bacterial expression of GST-HOIP variants (amino acids 1-480, 481-632, 633-1072, 633-909, or 910-1072), each cDNA was amplified by PCR with pEZ-M14/Flag-HOIP as a template and inserted into pGEX4T-1 (GE Healthcare Life Sciences). cDNA encoding human linear-Ub<sub>4</sub> was inserted into a GST fusion YA-GST-2 vector. A bacterial expression vector encoding MBP fusion protein of HOIP(910-1072) was constructed by subcloning cDNA corresponding to the LDD of human HOIP into pETDuet-1-MBP. The MBP-HOIP [910-1072 (S1066A, S1066E, or S1066D)] mutant constructs were prepared by site-directed mutagenesis with pETDuet-1-MBP-HOIP(910-1072) as template. The expression vectors for HA-TRAF2 variants (full-length or amino acids 272-501) were described previously (Roh and Choi, 2016). pGEX/hTNF $\alpha$ (77-233) was kindly provided by K. Iwai (Kyoto University, Japan). The cDNA encoding NEMO(257-346), which corresponds to the UBAN domain, was generated by PCR with pcMV5/Myc-NEMO as template and was inserted into *EcoRI* and *SaII* sites of pGEX-4T-1. Rabbit polyclonal antibodies to MST1 and to I $\kappa$ B $\alpha$ , rabbit monoclonal antibodies to phospho-p65 (Ser<sup>536</sup>), to phospho-IKK $\alpha$ / $\beta$  (Ser<sup>176</sup>/Ser<sup>180</sup>), to CYLD, and to A20, and mouse monoclonal antibodies to phospho-I $\kappa$ B $\alpha$  (Ser<sup>32/36</sup>) were from Cell signaling. Rabbit polyclonal antibodies to p65, to NEMO, to IKK $\alpha$ / $\beta$ , to the His<sub>6</sub> tag, to TRAF2, to TNFR1, and to GST as well as mouse monoclonal antibodies to GAPDH, to cIAP1, and to ubiquitin were from Santa Cruz Biotechnology (Santa Cruz, CA). Mouse monoclonal antibodies to RIP1, to the Flag epitope, and to NEMO/IKK $\gamma$  were from BD Transduction Laboratories, Sigma, and MBL (Nagoya, Japan), respectively. Rabbit polyclonal antibodies to HOIP and to HOIL-1L were from Abcam (Cambridge, UK), and rabbit polyclonal antibody to Sharpin was from Proteintech (Chicago, IL). Human antibody to linear ubiquitin was kindly provided by V. M. Dixit (Genentech, South San Francisco, CA). For detection of the phospho-Ser<sup>1066</sup> form of human HOIP, rabbit polyclonal phospho-specific antibodies were generated with a synthetic phosphorylated peptide (VPLGQpSIPRRR) as immunogen. Recombinant murine TNF $\alpha$  was obtained from Peprotech (Rocky Hill, NJ).

### Co-immunoprecipitation and immunoblot analysis

Cells were lysed in NETN lysis buffer [0.5% Nonidet P-40, 1 mM EDTA, 50 mM Tris-HCl, pH 8.0, 120 mM NaCl, 10 mM NaF, 1 mM phenylmethylsulfonyl fluoride, aprotinin (2  $\mu$ g/mL), leupeptin (2  $\mu$ g/mL)]. The lysates were incubated at 4°C for 16 h with appropriate antibodies and then for an additional 1 h in the presence of protein G-coupled agarose beads. The resulting precipitates were washed twice and then processed for SDS-PAGE. For immunoblot analysis, proteins on the gel were transferred to a polyvinylidene fluoride membrane and then probed with indicated primary antibodies. Immune complexes on the membrane were detected with horseradish peroxidase-conjugated secondary antibodies and enhanced chemiluminescence reagents (Thermo Fisher Scientific, Rockford, IL).

### Quantitative RT-PCR analysis

Total RNA was isolated from cultured cells with the use of TRIZOL reagent (Invitrogen). The RNA (1  $\mu$ g) was converted to cDNA by RT with an oligo(dT) primer. Real-time PCR was performed with an iQ5 thermocycler (BioRad) in a final volume of 20  $\mu$ L containing the synthesized cDNA, each primer (10  $\mu$ M), and 10  $\mu$ L of 2  $\times$  SYBR Green Supermix (Thermo Fisher Scientific). Each reaction was performed in triplicate, and data were analyzed with iQ5 optical system software (Bio-Rad). The amount of each target mRNA was normalized by that of GAPDH mRNA as an internal control. The sequences of the primers (forward and reverse, respectively) are as follows: IL-6, 5'-tctaattcatatctcaaccaagagg-3' and 5'-tggtccttagccactccttc-3'; I $\kappa$ B $\alpha$ , 5'-acgagcaaatggtgaaggag-3' and 5'-atgattccaagtcgagga-3'; GAPDH, 5'-cgtgcgcctggagaacc-3' and 5'-tggagagtgaggagtgctgtt-3'; iNOS 5'-atggagactgtccagcaat-3' and 5'-ggcgcagaactgagggta-3'.

### Mass Spectrometry of phosphoproteins

The active MST1 (0.5  $\mu$ g, Merk Millipore) was incubated for 30 min at 37°C with recombinant human HOIP(633-1072) (2  $\mu$ g) and 0.25 mM ATP in 20  $\mu$ L of a kinase reaction buffer, after which the reaction mixtures were processed with the Filter Assisted Sample Preparation (FASP) method (Wepf et al., 2009). In brief, the protein samples were dissolved in 9 M urea and subjected to reduction with 5 mM tris(2-carboxyethyl)phosphine (Sigma) at 60°C for 45 min and to alkylation with 20 mM C<sub>2</sub>H<sub>4</sub>INO (Sigma) at 25°C for 15 min. The samples were then cleaned with a 30-kDa Amicon Filter (UFC503096, Millipore) three times with the use of 9 M urea and twice

with 30 mM NH<sub>4</sub>HCO<sub>3</sub>. After proteolysis with trypsin (Promega) and chymotrypsin (Roche) at a 1: 20 ratio for 12 h at 37°C, the digested peptides were desalted and eluted with 0.1% trifluoroacetic acid in 60% acetonitrile. The extracted peptides were dried and then resuspended in 7  $\mu$ L of 0.1% formic acid for LC-MS/MS performed with an LTQ-Orbitrap Velos instrument (Thermo Fisher Scientific) interfaced with a nanoLC-2D and nanoACQUITY UltraPerformance LC system (Waters). Precursor and fragment ions were analyzed at a resolution of 30,000 and 7,500, respectively. Peptide sequences were identified from isotopically resolved masses in MS and MS/MS spectra extracted with and without deconvolution with the use of Thermo Scientific Xtract software. The data were analyzed with Proteome Discoverer 1.3 software (Thermo Scientific) configured with Mascot and Sequest search nodes and were searched against Refseq version 46 human entries with oxidation on Met, deamidation of Asn and Gln, and phosphorylation of Ser, Thr, or Tyr as variable modifications and carbamidomethylation of Cys as a fixed modification. Tolerances for precursor and fragment masses were set to 15 ppm and 0.03 Da, respectively. A peptide validator node was used for peptide confirmation, and a 1% false discovery rate cutoff was used to filter the data.

### Immune complex kinase assay

Cells were lysed in a lysis buffer (Ryoo et al., 2004) and assayed for MST1 activity with an immune complex kinase assay as previously described (Park et al., 2001; Ryoo et al., 2004) with myelin basic protein or HOIP fragments (1  $\mu$ g protein/assay) as substrates.

### In vitro binding assays

<sup>35</sup>S-labeled HOIP, Sharpin, HOIL-1L, and TRAF2 were produced *in vitro* with the use of a Quick Coupled TnT kit (Promega) and [<sup>35</sup>S]-methionine. The <sup>35</sup>S-labeled proteins were incubated for 1 h at 4°C in a binding buffer (Cho et al., 2003) with His<sub>6</sub>-MST1(K59R) and then for an additional 1 h in the presence of Ni-NTA beads (Incospharm, Korea). Bead-bound proteins were washed with buffer A (50 mM HEPES, pH 7.5, 150 mM NaCl, 1 mM EDTA, 1 mM dithiothreitol, 0.1% Tween 20) and then eluted with a solution containing 50 mM sodium phosphate buffer (pH 8.0), 300 mM NaCl, and 250 mM imidazole. Eluted <sup>35</sup>S-labeled proteins were subjected to SDS-PAGE and analyzed with a Fuji BAS 7100 phosphorimager (Fujifilm). For *in vitro* analysis of the binding of MST1 to HOIP fragments, His<sub>6</sub>-MST1(K59R) (6  $\mu$ g) was incubated for 1 h at 4°C with 4  $\mu$ g of GST, GST-HOIP(1-480), GST-HOIP(481-632), GST-HOIP(633-1072), GST-HOIP(633-909), or GST-HOIP(910-1072) in 500  $\mu$ L of binding buffer (Cho et al., 2003). The reaction mixtures were applied to glutathione-agarose beads (Incospharm), and bead-bound proteins were then eluted and subjected to immunoblot analysis with antibodies to the His<sub>6</sub> tag. For *in vitro* analysis of the binding of HOIP(633-909) to MST1 fragments, MST1 variants (Full-length, 1-326, and 327-487) were produced *in vitro* with using a Quick Coupled TnT kit and [<sup>35</sup>S]-methionine. The <sup>35</sup>S-labeled MST1 variants were incubated for 1 h at 4°C with GST or GST-HOIP(633-909) and for an additional 1 h in the presence of glutathione-agarose beads, and then the bead-bound proteins were eluted and subjected to SDS-PAGE and analyzed with a Fuji BAS 7100 phosphorimager (Fujifilm), as described above. For *in vitro* analysis of the ubiquitin-HOIP(LDD) interaction, MBP or WT or S1066A mutant forms of MBP-HOIP(LDD) (2  $\mu$ g each) was incubated for 1 h at 30°C in 20  $\mu$ L of a kinase reaction buffer in the absence or presence of recombinant active MST1 protein. After *in vitro* kinase reaction, the reaction mixtures were incubated for 1 h at 4°C with 2  $\mu$ g of GST-linear Ub<sub>4</sub> in 500  $\mu$ L of binding buffer and were then subjected to pull down with glutathione-agarose beads. Bead-bound proteins were analyzed by immunoblotting with antibodies to MBP.

### In vitro ubiquitination assays

HEK293 cells were transfected for 48 h with expression vectors for Flag-HOIP and Myc-HOIL-1L, and the cell lysates were immunoprecipitated with anti-Flag antibody. *In vitro* ubiquitination assays were performed by incubating the Flag-immunoprecipitates at 37°C for 1 h with 30  $\mu$ L of a reaction buffer (50 mM Tris-HCl, pH 7.6, 5 mM MgCl<sub>2</sub>, 2 mM dithiothreitol, 2 mM ATP) supplemented with 2  $\mu$ g of ubiquitin (Sigma), 12 ng of E1 (Boston Biochem), and 200 ng Ubch5c (Millipore, Billerica, MA). The reaction mixtures were then subjected to SDS-PAGE and immunoblot analysis with antibodies to ubiquitin or to linear ubiquitin chains. For *in vitro* analysis of the effect of MST1-catalyzed HOIP phosphorylation on the E3 activity of HOIP, 2  $\mu$ g of His<sub>6</sub>-MBP-HOIP (699-1072) (Abcam) was incubated for 1 h at 30°C in 20  $\mu$ L of a kinase reaction buffer in the absence or presence of 2  $\mu$ g recombinant active MST1 protein (Millipore). After *in vitro* kinase reaction, the reaction mixtures were incubated for 1 h at 37°C in 20  $\mu$ L of the reaction buffer containing 12 ng of E1 and 200 ng Ubch5c in the absence or presence of 2  $\mu$ g of ubiquitin, and then analyzed by immunoblotting with antibodies to ubiquitin.

### Pull-down assay of linear ubiquitin chains using GST-fused M1-SUB

Cells were lysed in a lysis buffer [20 mM Sodium phosphate, pH 7.4, 1% Nonidet P-40, 2 mM EDTA, 1 mM dithiothreitol, 5 mM N-ethylmaleimide, 10 mM NaF, 1 mM phenylmethylsulfonyl fluoride, aprotinin (2  $\mu$ g/mL), and leupeptin (2  $\mu$ g/mL)], and the lysates were subjected to pull down with GST-fused M1-SUB, as previously described (Keusekotten et al., 2013).

### Immunofluorescence analysis

MEFs were grown on glass coverslips in six-well culture plates, fixed with 3% formaldehyde, permeabilized with 0.25% Triton X-100, blocked with 10% horse serum, and then incubated overnight at 4°C with goat anti-TNF $\alpha$ , rabbit anti-linear ubiquitin chain, or rabbit anti-K63 ubiquitin antibodies, as indicated. They were additionally incubated for 2 h at room temperature with fluorescein isothiocyanate (FITC)-conjugated anti-goat and Texas red-conjugated anti-rabbit secondary antibodies (Vector Laboratories), followed by

nuclear staining with DAPI. The fluorescent images were visualized with a LSM 800 confocal laser scanning microscope (Carl-Zeiss) and processed with ZEN software 2012 (Carl-Zeiss).

### **In situ PLA**

An *in situ* PLA was performed as described previously (Roh and Choi, 2016). In brief, MEFs were grown on glass slides in six-well culture plates, fixed, permeabilized, blocked with 10% FBS, and then incubated overnight at 4°C with antibodies to Flag and to Myc. The cells were then subjected to the *in situ* proximity ligation reaction with PLA probes (Olink Bioscience) and examined by confocal fluorescence microscopy. Fluorescence images were processed with ZEN software 2012 (Carl-Zeiss).

### **RNAi**

Small interfering RNAs (siRNAs) specific for mouse HOIP mRNA and a scrambled control siRNA were synthesized by Invitrogen. The two nonoverlapped HOIP siRNAs (si-HOIP-1 and -2) were targeted to the sequences 5'-GAGGACGGAGUUGUGAGGAAUUUCCA-3' and 5'-CUGCUAAGAGAGAGCGUUGAAGAUG-3', respectively. The scrambled control siRNA (si-sc) was targeted to the sequences 5'-GAGGGCUGAUGUGAGUAGUUGACCA-3'. The mouse MST2 siRNA (si-MST2) and a scrambled control siRNA were targeted to the sequences 5'-CCCAUGAUGGAACGAGAAAUA-3' and 5'-CGUACGCGAAUACUUCGAUU-3', respectively. Cultured cells were transfected with siRNA duplexes with the use of Lipofectamine RNAiMAX (Invitrogen, Carlsbad, CA).

### **Analysis of TNF-RSC**

MEFs were left untreated or treated with GST-TNF $\alpha$  (1  $\mu$ g/mL) for the indicated times and then lysed in NETN lysis buffer. The lysates were incubated for 2 h at 4°C with glutathione-agarose beads. Cell lysates from the untreated control cells were mixed with GST-TNF $\alpha$  (0.1  $\mu$ g) during incubation with the beads, to monitor non-specific binding to GST-TNF $\alpha$ . Bead-bound proteins were pulled down and washed twice with the lysis buffer. The resulting TNF-RSC precipitates were subjected to immunoblot analysis with the indicated antibodies. For immunoprecipitation of MST1 from the isolated TNF-RSC, the bead-bound proteins were eluted with 6 M urea buffer [6 M urea, 50 mM Tris-HCl, pH 8.0, 120 mM NaCl, 1.5 mM MgCl<sub>2</sub>, 1 mM EGTA, 1% Triton X-100, 10 mM NaF, 10 mM  $\beta$ -glycerophosphate, 1 mM Na<sub>3</sub>VO<sub>4</sub>, 1 mM phenylmethylsulfonyl fluoride, aprotinin (2  $\mu$ g/mL), leupeptin (2  $\mu$ g/mL)], diluted 1:1 with NETN lysis buffer, and then immunoprecipitated with anti-MST1 antibody. The resulting immunoprecipitates were analyzed by immunoblotting with the indicated antibodies.

### **pIMAGO-based detection of phosphorylated proteins**

Cells were lysed in NETN lysis buffer, and the lysates were immunoprecipitated with antibody to HOIP. The resulting precipitates were washed twice with the lysis buffer, processed for SDS-PAGE, and then examined for the phosphorylation of HOIP with the use of a pIMAGO kit (Tymora Analytical Operations).

### **Nuclear fractionation and NF- $\kappa$ B p65 ELISA**

A nuclear fraction prepared from cultured cells as previously described (Yun et al., 2011) was examined for the DNA binding activity of the p65 subunit of NF- $\kappa$ B with the use of an enzyme-linked immunosorbent assay (ELISA) kit (TransAM NF $\kappa$ B Kit, Active Motif).

### **IL-6 ELISA**

MEFs or primary BMDMs were incubated in absence or presence of TNF $\alpha$  (20 ng/mL) for the indicated times, after which culture supernatants were collected and assayed for IL-6 or TNF $\alpha$  with an ELISA kit (eBioscience).

### **Administration of TNF $\alpha$**

Eight-week-old C57BL/6 mice were injected intraperitoneally with recombinant murine TNF $\alpha$  (125  $\mu$ g/kg). After 5 h of the injection, the mice were anaesthetized and intracardially perfused with PBS. Lung tissues were dissected and examined for co-immunoprecipitation and immunoblot analysis.

### **Statistical analysis**

Quantitative data are presented as means  $\pm$  SEM and were analyzed by Student's *t* test. A *P* value of < 0.05 was considered statistically significant.

### **DATA AND SOFTWARE AVAILABILITY**

Raw data were deposited to Mendeley data at: <https://doi.org/10.17632/d5k5jv8ygt.1>.